Expectation generation and its effect on subsequent pain and visual perception

Rotem Botvinik-Nezer[1,2,*], Stephan Geuter[3], Martin A. Lindquist[3] and Tor D. Wager[2,*]

[1]Hebrew University of Jerusalem; [2]Dartmouth College; [2]Johns Hopkins University;

[*]Corresponding authors

Abstract

Bayesian accounts of perception, such as predictive processing, suggest that perceptions integrate expectations and sensory experience, and thus assimilate to expected values. Furthermore, more precise expectations should have stronger influences on perception. We tested these hypotheses in a paradigm that manipulates both the mean value and the precision of cues within-person. Forty-five participants observed cues–presented as ratings from 10 previous participants–with varying cue means, variances (precision), and skewness across trials. Participants reported expectations regarding the painfulness of thermal stimuli or the visual contrast of flickering checkerboards. Subsequently, similar cues were each followed by a visual or noxious thermal stimulus. While perceptions assimilated to expected values in both modalities, cues' precision mainly affected visual ratings. Furthermore, behavioral and computational models revealed that expectations were biased towards extreme values in both modalities, and towards low-pain cues specifically. fMRI analysis revealed that the cues affected systems related to higher-level affective and cognitive processes–including assimilation to the cue mean in a neuromarker of endogenous contributions to pain and in the nucleus accumbens, and activity consistent with aversive prediction-error-like encoding in the periaqueductal gray during pain perception–but not systems related to early perceptual processing. Our findings suggest that predictive processing theories should be combined with mechanisms such as selective attention to better fit empirical findings, and that expectation generation and its perceptual effects are mostly modality-specific and operate on higher-level processes rather than early perception.

Introduction

Current theories of perception, such as Bayesian theories [1,2] and predictive processing [3,4], posit that the brain represents the world with an internal generative model, used to predict future external (sensory input) and internal (physiological states) events. Model and cue-based expectations (prior beliefs) computationally combine with incoming sensory information (likelihoods) to form perceptions (posterior beliefs) [5,6]. In line with this principle, predictions about upcoming stimuli have been shown to shape their perception across sensory modalities. For example, reported painfulness of noxious stimuli assimilates to expected values [7–12]. Likewise, the perceived direction of randomly moving dots is biased towards expected directions [5,13,14]. Such assimilation is beneficial, as it improves perception when contextual information is relevant. Similar Bayesian principles have been suggested to underlie interoception [15–17] and diverse aspects of cognition [18,19] including planning and decision-making (e.g., active inference [20,21]). However, such models also have contrastive mechanisms, which drive learning. While assimilation of perceptions to predicted values is one way to resolve discrepancy between predictions and sensory input, another important way is to update the predictive model to match the input, i.e., to learn. Prediction error (PE)-driven updating is a crucial form of learning. However, which brain signals assimilate to expectations, perhaps forming a neural substrate for perception, and which encode PEs and thus drive learning, is a topic of active investigation.

Bayesian models of predictive processing make predictions about how the relative precision of cues and sensory stimuli affects perception and neural responses. Prior predictions and likelihoods (i.e., the expectation and the incoming sensory information) are weighted by their relative precision [2,5,6,22–24]. Thus, Bayesian models predict an interaction between the expected value and its precision, such that more certain expectations (prior beliefs) should affect perception (posterior beliefs) more strongly. This hypothesis has been supported by studies on pain perception showing stronger placebo analgesia in individuals with more precise treatment expectations [25,26], and greater assimilation of perceived pain towards expectations with higher cue precision [27,28]. Conversely, other studies have found that lower precision or predictability (higher uncertainty) leads to more pain, putatively because uncertainty is aversive in the context of potential harmful stimuli [7,29]. Finally, some other studies did not replicate these effects and even found instead that more certain cues led to more pain [30–34]. The contradicting findings regarding the effect of the cue certainty on

pain perception [35] may stem from differences across experimental designs (e.g., how precision was manipulated, or the rating scale that was used), sensory modalities (e.g., uncertainty may be particularly aversive in the context of painful stimuli given the threat they pose), and / or participant populations (e.g., individual differences in the aversiveness of uncertainty, or participants' beliefs about the information they are given and thus their generated expectations).

A promising paradigm, which we adopt here, uses cues with rich information about the distribution of predicted values, allowing within-person manipulation of precision and other distributional properties [7,8,10,27,30]. This can substantially increase power and reduce confounds in testing manipulations of precision. The version that we use presents multiple-valued cues as ratings of multiple previous participants (Figure 1), providing an additional advantage in that it provides a plausible type of social observational learning that may be particularly impactful [36–41]. Though such cues have been used successfully in multiple studies, an additional complexity is that manipulation of the cues' precision–i.e., the variance of the presented cue values–influences other properties, including the maximum and minimum values. If people weight all cue values equally, this is ignorable, but participants may instead attend to the highest or lowest values, depending on the task and their predispositions (e.g., if some participants find pain to be threatening and are vigilant for high-pain cues).

Such effects are not taken into consideration in most studies testing Bayesian accounts of perception, but there is evidence that they can be important. For instance, a previous study in visual perception has demonstrated overweighting of inliers (values closer to the mean) [42]. Such effects may also be sensitive to the precise demands of the task. For example, when asked to determine which series of numbers was on average larger, people have been found to overweight outliers (extreme values), and specifically larger values [43]. Furthermore, this kind of nonlinear weighting might depend on the sensory modality, and has not been studied in the context of pain perception. If attention to extreme values is related to vigilance for potential threat, people might weight them more strongly for pain than for other, safer modalities. This could, in principle, explain previous findings of higher pain ratings following less precise cues [7]: If people are biased towards maximal pain values ("danger signals"), and higher variance entails larger maximal values, then this effect is expected.

Moreover, pain perception is considered more subjective and ambiguous compared to other types of perception, like perception of visual contrast. Thus, its likelihood might be less precise, and predictive cue effects might be increased compared to other modalities. If this is the case, it suggests that the nature of the predictive processes at play are at least to some degree modality-specific, and theories of perception must identify differences and commonalities across different types of sensory input [23].

Finally, it is still unclear how expectations, and their precision, influence brain processes underlying pain and visual perception. Some evidence suggest that influences of expectations can reach the earliest stages of sensory processing, for example in the spinal cord [44–46], cortical nociceptive pain processing regions [9,47], and primary visual cortex [14,48]. Other studies show that expectations modulate higher-level affective and cognitive processes [49,50]. However, others have questioned how strongly context-based influences affect perception [51]. Moreover, we have recently shown that placebo treatment (which is thought to operate via expectation modulation, among other effects [52–54]) induces analgesia via modulation of affective and cognitive processes, rather than nociceptive pain processing [55]. If expectation effects mostly operate via high-level affective and cognitive processes, they should be reduced for basic perception that is not subject to affective evaluation, like brightness or visual contrast. Alternatively, these processes could be mediated by different mechanisms across modalities, and thus subject to different behavioral influences and related to different patterns of neural activity.

Here, we test how expectations are generated from distribution cues with varying levels of mean, variance, and skewness (and thus the presence and direction of outliers), and how they affect subsequent perception of visual and painful stimuli (for the study design and illustration of the cues see Figure 1 and Methods). The cues were not externally reinforced and were not predictive of subsequent stimuli. By comparing pain and visual perception, we identify common and distinct mechanisms for expectation formation and modulation of perception for stimuli that are potentially harmful and more ambiguous (painful) and those that are non-harmful and less ambiguous (visual). Using fMRI and a priori neuromarkers and individual regions of interest (ROIs), we test whether and how neural responses during pain and visual perception are affected by the different properties of the cue and by the cue-based expectations.

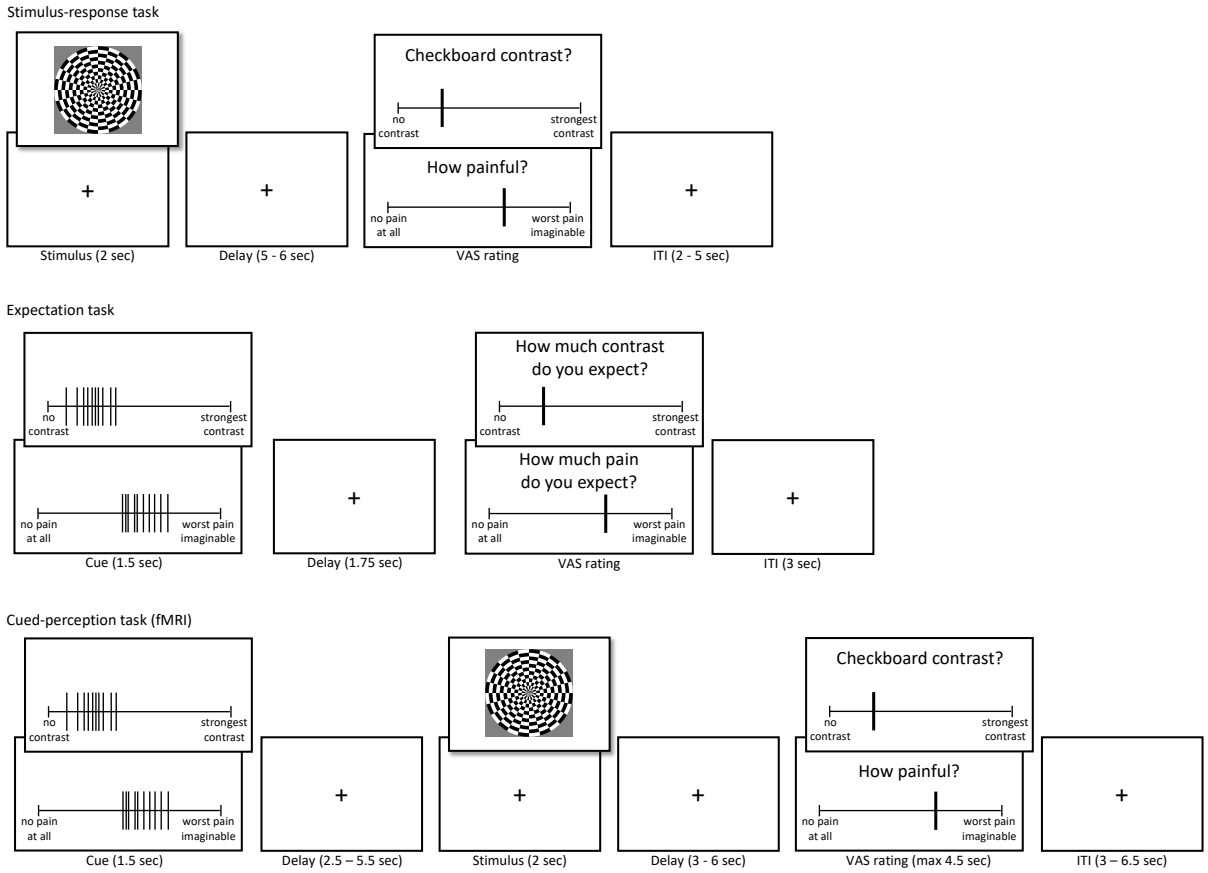

Figure 1. Experimental design. An illustration of the three experimental tasks: stimulus-response task (top panel), expectation task (middle panel), and cued-perception task (bottom panel; performed during an fMRI scan). When two rectangles are presented on top of each other (e.g., for the ratings in all tasks), the lower one illustrates pain trials and the upper one illustrates visual trials.

Results

In the first task, participants rated the painfulness of thermal stimuli and the visual contrast of flickering checkerboards with different intensities (Figure 1). Data from this task verified that participants' ratings were higher for higher stimulus intensity levels in both modalities (linear mixed-effects model: pain: $\beta = 0.633$, $SE = 0.028$, $t_{(44)} = 22.43$, $p < .001$; vision: $\beta = 0.868$, $SE = 0.018$, $t_{(44)} = 47.59$, $p < .001$).

Expectation generation from distribution cues

In the expectation task, participants were presented with the distribution cues, and rated their expectations regarding noxious and visual stimuli following each cue (stimuli were not delivered during this task).

Effects of cue mean on expectations. Expectation ratings significantly assimilated to the cues' mean (linear mixed-effects model: $\beta = 0.907$, $SE = 0.015$, $t_{(50)} = 59.14$, $p < .001$; Figure 2A). This effect did not interact with modality ($\beta = -0.006$, $SE = 0.005$, $t_{(16000)} = -1.26$, $p = .210$), and was found for each modality separately (pain: $\beta = 0.901$, $SE = 0.015$, $t_{(57.7)} = 62.72$, $p < .001$; vision: $\beta = 0.913$, $SE = 0.021$, $t_{(51.3)} = 43.25$, $p < .001$).

Effects of cue variance on expectations. Previous studies have mostly focused on the effect of cues' variance on perception rather than expectations, as the variance should influence the precision (certainty) of the expectations, not their value. Here, the cue variance did not significantly affect expectation ratings across both modalities ($\beta = -0.021$, $SE = 0.010$, $t_{(59.83)} = -1.994$, $p = .051$; Figure 2A), but there was a significant cue mean x modality interaction ($\beta = -0.024$, $SE = 0.005$, $t_{(16000)} = -5.01$, $p < .001$): Expectation ratings were significantly higher for lower cue variance in pain trials ($\beta = -0.045$, $SE = 0.014$, $t_{(58.1)} = -3.16$, $p = .002$), but not in vision trials ($\beta = 0.004$, $SE = 0.013$, $t_{(66)} = 0.25$, $p = .802$). In other words, participants expected more painful stimuli after more certain cues, but this was not true for noxious stimuli. This finding is inconsistent with both the Bayesian predictive processing account and the alternative account of uncertainty aversiveness. We further tested the interaction between the effects of cue mean and variance on subsequent ratings, which based on Bayesian predictive processing accounts is expected to be significant for stimulus, and not expectation, ratings. Indeed, the cue mean x variance interaction was not significant in either modality (pain: $\beta = -0.0002$, $SE = 0.006$, $t_{(7956)} = -0.026$, $p = .979$; vision: $\beta = 0.014$, $SE = 0.007$, $t_{(7956)} = 1.93$, $p = .053$).

Effects of cue skewness on expectations. We tested for the first time how the skewness of the cue distribution affects expectations. We reasoned that previous studies that have manipulated the cue variance also altered extreme values, and that people might be biased towards such values, particularly in the context of threat (i.e., on pain trials). Here, extreme values indeed biased participants' expectations, which were higher for positively skewed compared to symmetric cues

(β = 0.028, SE = 0.007 , $t_{(16000)}$ = 4.11, p < .001; Figure 2B) and lower for negatively skewed compared to symmetric cues (β = -0.050, SE = 0.007 , $t_{(16000)}$ = -7.38, p < .001). These effects were also significant in each modality separately (pain, negative vs. symmetric: β = -0.064, SE = 0.009, $t_{(7956)}$ = -7.13, p < .001; pain, positive vs. symmetric: β = 0.032, SE = 0.009 , $t_{(7956)}$ = 3.59, p < .001; vision, negative vs. symmetric: β = -0.037, SE = 0.010 , $t_{(7956)}$ = -3.77, p < .001; vision, positive vs. symmetric: β = 0.024, SE = 0.010 , $t_{(7956)}$ = 2.45, p = .014). These findings are consistent with over-weighting of extreme values when constructing expectations.

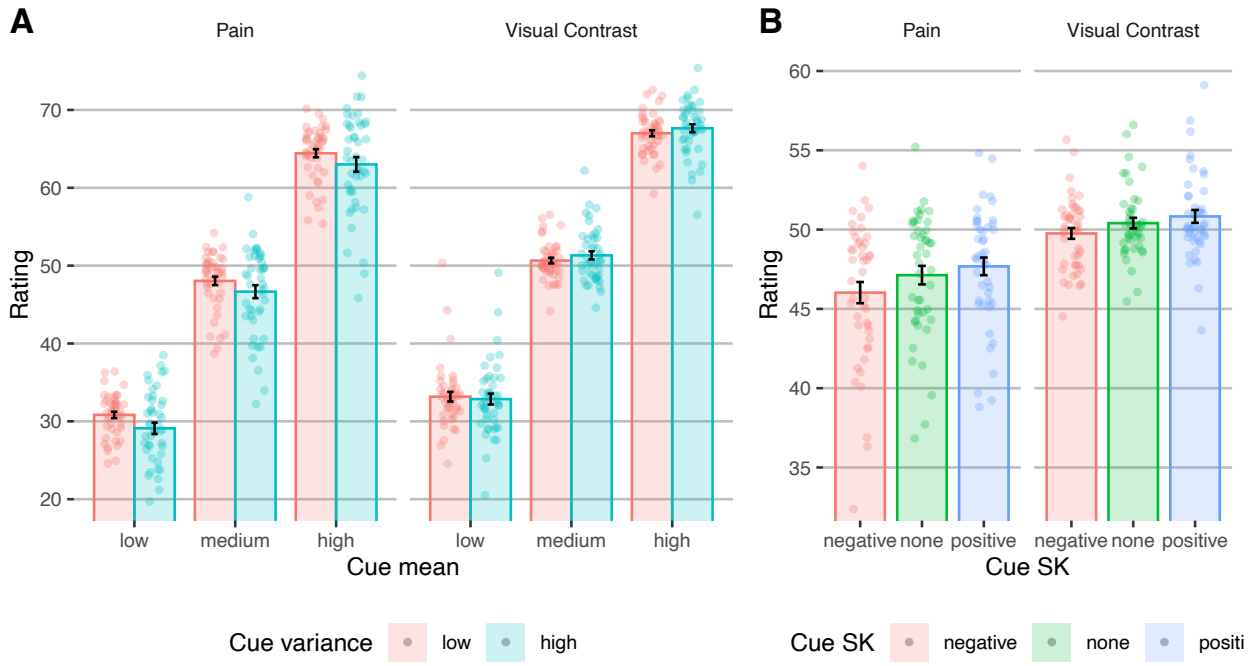

Figure 2. Behavioral results - expectation task. (**A**) Participants' expectation ratings as a function of the mean (five cue mean levels were collapsed into three for visualization) and variance of the cue's values, in pain and vision trials. (**B**) Participants' expectation ratings as a function of the skewness of the cue's values, in pain and vision trials. In both panels, bars represent averages across participants, error bars represent the standard error of the mean across participants, and points represent single participants.

In addition, expectation ratings were significantly higher in vision compared to pain trials (Vision: M = 50.33, SE = 0.319; Pain: M = 46.945, SE = 0.586; β = -0.094, SE = 0.020 , $t_{(47.8)}$ = -4.82, p < .001). This result suggests that participants might have been biased by lower values particularly in the context of pain, or viewed themselves as less sensitive to pain compared to other participants. Finally, there was a significant cue variance x cue skewness interaction (β = 0.021, SE = 0.007, $t_{(16000)}$ = 3.064, p = .002), indicating that lower extreme values affected expectations more when there was overall stronger agreement (less variance) among the cue values.

Overall, the behavioral results of the expectation task suggest that extreme values bias expectations, and that participants were particularly attentive to lower extreme values, mostly in the context of pain.

Computational model: weighting of cue values. To more directly test whether participants weight all cue values equally or overweight particular values (e.g., inliers vs. outliers, or smaller vs. larger values), we developed a computational model of expectation generation. The model assumes that in each cue, each value is weighted based on its relative location in the distribution of the 10 values (Figure 3A). Each value's weight is based on a combination of a power term modeling the weighting of inliers vs. outliers with the free parameter k, and a logistic term modeling the weighting of values that are smaller vs. larger than the mean with the free parameter b (see Methods for a detailed description). The model was largely inspired by the model of Spitzer et al. in the context of numeric estimation [43].

We fit the model to the expectation data to estimate the two free parameters, k and b for each modality and participant. The expectation model fit the data well overall, with an average correlation between predicted and empirical expectation ratings across participants of Pearson's $r = 0.945$ ($SD = 0.032$) for pain and $r = 0.928$ ($SD = 0.074$) for vision, and an average root mean squared error (RMSE) of 5.904 ($SD = 1.668$) for pain and 6.415 ($SD = 2.545$) for vision (on a rating scale of 0-100). This indicates that participants tracked variation in cues accurately, and that the model predicted their responses well and performed generally better in pain than in vision (Figure 3B).

The free parameter k measures over-weighting of inliers ($k > 1$) or over-weighting of outliers ($k < 1$), while b measures over-weighting of values that are smaller ($b < 0$) or larger ($b > 0$) than the mean value. We found that participants significantly over-weighted outliers in both modalities (i.e., $k > 1$; Wilcoxon signed rank test; Pain: median $k = 1.66$, $p = .019$; Vision: median $k = 1.47$, $p = .008$), and also smaller values specifically in pain and not in vision (i.e., $b < 0$; Wilcoxon signed rank test; Pain: median $b = -1.64$, $p < .001$; Vision: median $b = 0.16$, $p = .446$). Furthermore, k values, but not b values, were correlated between the two modalities across participants (Spearman correlation; k: $\rho = 0.45$, $p = .002$; b: $\rho = 0.16$, $p = .304$).

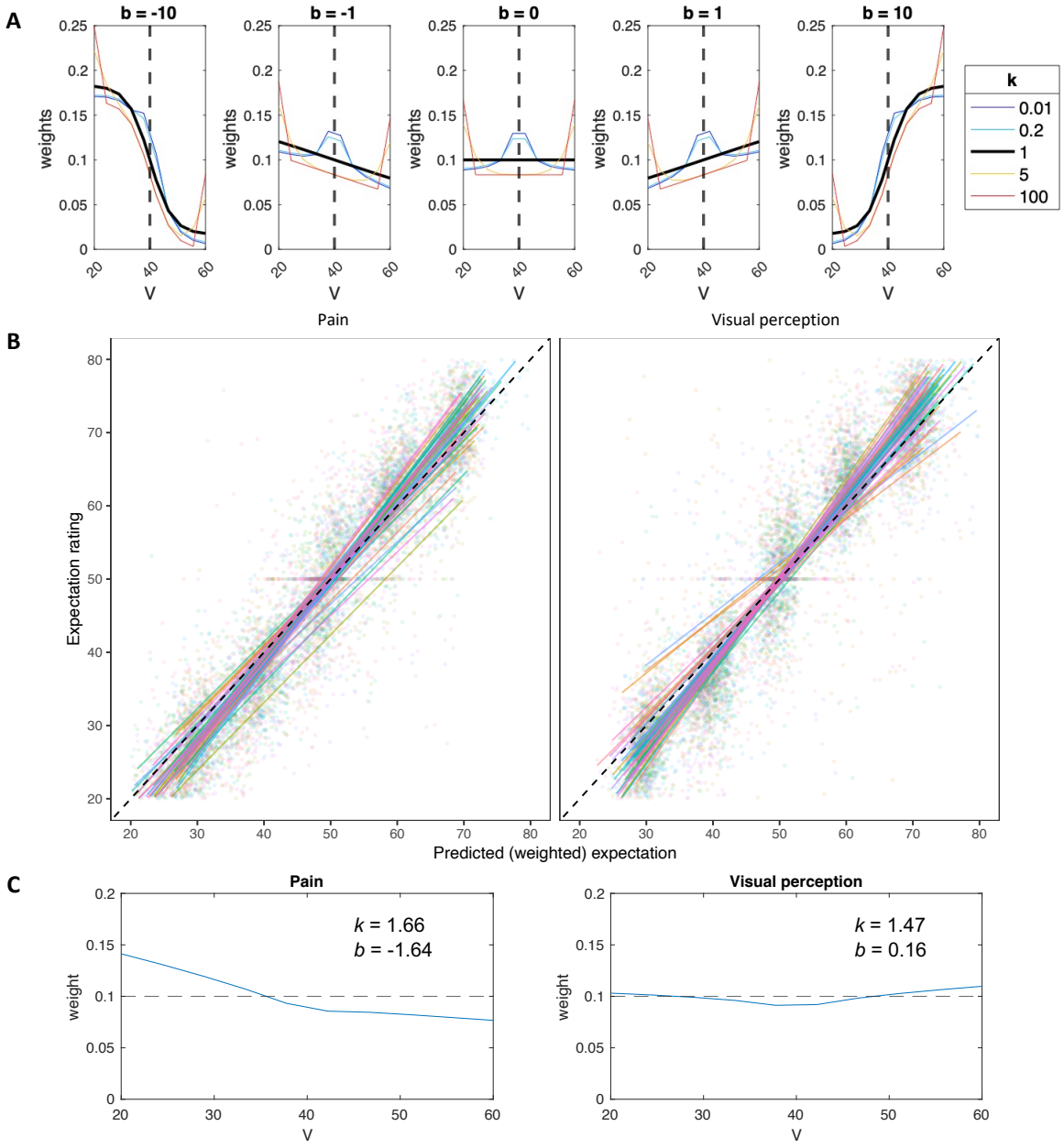

Figure 3. Computational model of expectation generation. (**A**) Simulations of the expectation model: Mapping of cue values, V (10 per cue), to weights for expectation computation, based on the two free parameters of the model: k and b. When $k = 1$ (black line), inliers and outliers are equally weighted. When $k < 1$ (cold colors), inliers are over-weighted, and when $k > 1$ (hot colors), outliers are over-weighted. When $b < 0$ (left panels), values below the mean are over-weighted, when $b > 0$ (right panels) values above the mean are over-weighted, and when $b = 0$ (middle panel), values are equally weighted. The dashed line represents the cue mean. (**B**) Correlations between the observed and predicted (based on the computational model) expectation ratings were very high across participants. Each line represents a single participant, and each dot represents a single trial. Data from different participants are presented in different colors. (**C**) The weight function for each modality, based on the median k and b values across the group. The dashed line represents equal rating of all cue values (V). Note that panels A and C are based on a symmetric cue consisting of equally distributed values between 20 and 60.

Finally, we tested whether the estimated *k* and *b* values correlated with state / trait scores based on questionnaires completed by the participants prior to the cued-perception task. For example, people with higher fear of pain, pain catastrophizing, or anxiety may focus more on cues predicting higher expected pain. However, all correlations between the available measures in our sample (Fear of Pain score [56], Pain Catastrophizing score [57], and State-Trait Anxiety Inventory score [58]) and optimized *k* or *b* for each modality across participants, were not significant (Fear of Pain: *k* pain $r = 0.16$, $p = .284$, *k* vision $r = 0.04$, $p = .800$, *b* pain $r = 0.22$, $p = .140$, *b* vision $r = 0.03$, $p = .825$; Pain Catastrophizing: *k* pain $r = -0.17$, $p = .267$, *k* vision $r = 0.09$, $p = .553$, *b* pain $r = 0.08$, $p = .582$, *b* vision $r = 0.06$, $p = .705$; State Anxiety: *k* pain $r = 0.15$, $p = .32$, *k* vision $r = 0.13$, $p = .402$, *b* pain $r = 0.05$, $p = .734$, *b* vision $r = -0.02$, $p = .905$).

Taken together, the behavioral and computational results of the expectation task suggest that while expectations strongly assimilate towards the mean cue value, participants overweight extreme cue values in both modalities, and demonstrate an optimism bias specifically in pain, relying more on low than high extreme values. Such effects were not considered in most previous studies, and could potentially explain the inconsistent results with regard to the effect of expectation variance on pain perception, if extreme values were unintentionally manipulated along with the uncertainty.

The effects of cue-based expectations on perception

In the cued-perception task (Figure 1), participants viewed cues followed by painful heat or flickering checkerboards. As expected, participants rated stimuli with higher intensity levels (higher temperature or visual contrast) as more intense ($\beta = 0.322$, $SE = 0.016$, $t_{(5856)} = 20.46$, $p < .001$). This effect was also significant for each modality separately (pain: $\beta = 0.323$, $SE = 0.027$, $t_{(129.6)} = 11.838$, $p < .001$; visual perception: $\beta = 0.333$, $SE = 0.032$, $t_{(88.8)} = 10.552$, $p < .001$).

Effects of cue mean on perception. Participants' stimuli ratings assimilated to the cue mean ($\beta = 0.253$, $SE = 0.033$, $t_{(61.5)} = 7.693$, $p < .001$; Figure 4A), replicating previous studies. This effect was significant for both pain ($\beta = 0.230$, $SE = 0.036$, $t_{(81.44)} = 6.443$, $p < .001$) and visual perception ($\beta = 0.289$, $SE = 0.039$, $t_{(69.6)} = 7.503$, $p < .001$), and cue mean effects on pain and visual perception were correlated across participants (Pearson's r = 0.82, $t_{41} = 9.174$, 95% CI = [0.689, 0.899], $p < .001$), indicating that participants who were affected by the cues were similarly affected in both modalities.

Effects of cue variance on perception. Participants rated stimuli with higher cue variance as more intense (β = 0.037, *SE* = 0.016 , $t_{(5857)}$ = 2.320, p = .020). This finding is consistent with Yoshida et al., [7], who suggested that uncertainty is aversive in the context of pain and thus lead to higher pain ratings, although a direct replication did not find this effect [30]. The modality x cue variance interaction was not significant (β = -0.137, *SE* = 0.016, $t_{(5858)}$ = -0.869, p = .385). However, when tested separately, it was only significant for visual (β = 0.060, *SE* = 0.021, $t_{(2877)}$ = 2.837, p = .005) and not for pain stimuli (β = 0.021, *SE* = 0.022 , $t_{(2846)}$ = 0.928, p = .354), which does not support the hypothesis that uncertainty is aversive particularly in the context of harmful stimuli.

As described above, Bayesian predictive processing accounts predict that the effect of the cue mean (expectation value) on perception should be smaller with higher cue variance (lower expectation precision). In line with this prediction, across modalities, the effect of the cue mean was smaller when the cue variance was higher (cue mean *x* variance interaction: β = -0.044, *SE* = 0.016 , $t_{(5859)}$ = -2.828, p = .005). This effect did not interact with modality (β = 0.003, *SE* = 0.016 , $t_{(5857)}$ = 0.212, p = .832), but when tested separately, it was only significant for visual stimuli (β = -0.056, *SE* = 0.021 , $t_{(2878)}$ = -2.661, p = .008) and not for pain (β = -0.036, *SE* = 0.022 , $t_{(2850)}$ = -1.594, p = .111).

Effects of cue skewness on perception. Ratings were higher when they were preceded by positively skewed compared to symmetric cues (β = 0.046, *SE* = 0.022, $t_{(5857)}$ = 2.052, p = .040; Figure 4B), but were not lower following negatively skewed compared to symmetric cues (β = -0.034, *SE* = 0.022 , $t_{(5857)}$ = -1.547, p = .122). The modality x skewness interactions were not significant (negative vs. symmetric: β = -0.002, *SE* = 0.022 , $t_{(5857)}$ = -0.104, p = .917; positive vs. symmetric: β = -0.032, *SE* = 0.022 , $t_{(5857)}$ = -1.421, p = .155). However, when tested separately, the skewness only affected visual perception (higher ratings after positively skewed vs. symmetric cues; β = 0.092, *SE* = 0.030, $t_{(2878)}$ = 3.086, p = .002; no significant effect for negatively skewed vs. symmetric cues, β = -0.038, *SE* = 0.030, $t_{(2876)}$ = -1.276, p = .202) and not pain (negative vs. symmetric: β = -0.033, *SE* = 0.032 , $t_{(2845)}$ = -1.038, p = .299; positive vs. symmetric: β = 0.012, *SE* = 0.032 , $t_{(2845)}$ = 0.377, p = .706).

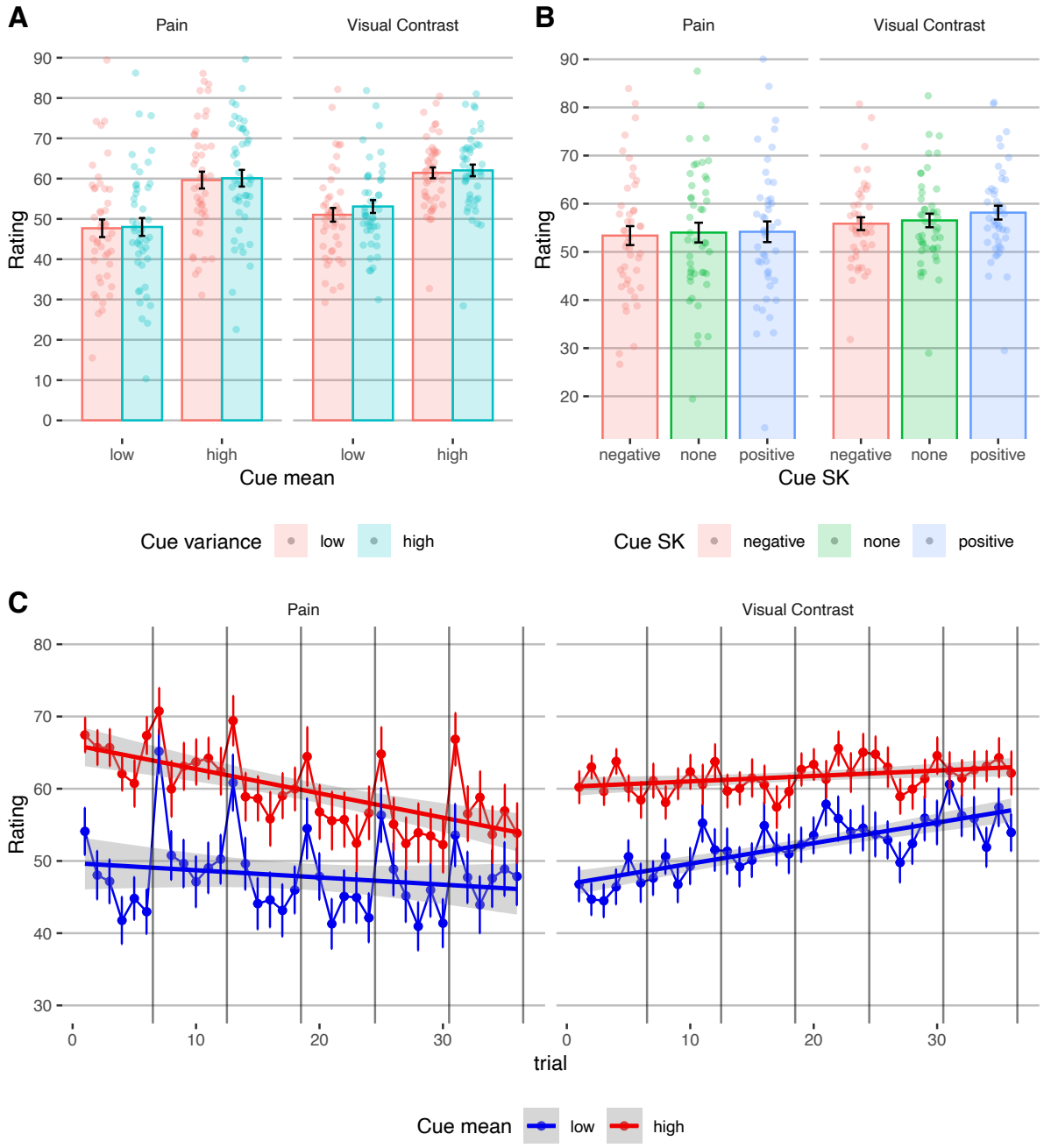

Figure 4. Behavioral results, cued-perception task. (**A**) Participants' perception ratings as a function of the mean (x axis) and variance (color) of the cue's values, in pain and visual trials (column). (**B**) Participants' perception ratings as a function of the skewness (x axis and color) of the cue's values, in pain and visual trials (columns). In panels A and B, bars represent averages across participants, error bars represent the standard error of the mean across participants, and points represent single participants. (**C**) The effect of the cue mean (color) on pain and visual contrast ratings over time, in pain and visual perception (columns). Error bars represent standard error of the mean across participants. The lines represent the linear fit, and the gray shading represents 95% CIs of the linear fit. Vertical major grids separate between different runs (note that a new skin site was used for each run, and thus the increase in the averaged pain rating for the first trial of each run stems from site-nonspecific sensitization and site-specific habituation[59]).

Overall, ratings were higher following cues with higher mean, higher variance, or positive skewness, suggesting that extreme positive values carry more influence on perception. Surprisingly, however, effects of the cue precision and extreme values on perception were mostly found in visual rather than pain perception, inconsistent with the idea that uncertainty enhances threat. In line with Bayesian predictive processing accounts, the cue mean influenced perception more when the cues were more precise. However, predictive processing accounts do not explain why the ratings were also higher following higher uncertainty, and why the cue precision was not a significant factor in pain perception. Finally, computational modeling indicated that perception assimilates towards expected values more in pain compared to visual perception, in line with the hypothesis that pain perception is more ambiguous and thus more sensitive to contextual information (see Supplementary Results - Computational Modeling of Perception).

Does the effect of cue-based expectation persist? The interaction between the trial number and the cue mean effect was not significant (Figure 4C; both modalities: β = -0.009, SE = 0.011 , $t_{(5918)}$ = -0.816, p = .414; pain: β = -0.002, SE = 0.015 , $t_{(2903)}$ = -0.115, p = .908; visual perception: β = -0.010, SE = 0.015 , $t_{(2948)}$ = -0.669, p = .503), and the cue mean effect was significant on the last trial (t_{81} = -3.18, mean difference 95% CI = [-13.427, -3.101], p < .001), demonstrating a persistent cue effect. Computational modeling strengthened the conclusion that most participants did not learn to ignore the cues during the task (see Supplementary Results - Computational Modeling of Perception), in line with previous studies [9,60–62].

Cue and stimulus intensity effects on neural processing

Effects on pain neuromarkers. We focused on two *a priori* neuromarkers for pain (Figure 5A): (1) The Neurologic Pain Signature (NPS [63]), which is sensitive and specific to nociceptive pain across studies, tracks the intensity of nociceptive input, and predicts pain ratings with very large effect sizes in >50 published study cohorts [49,64]. (2) The Stimulus Intensity Independent Pain Signature (SIIPS [65]), which captures higher-level, endogenous influences on pain construction independent of stimulus intensity and the NPS score. In most previous studies, the NPS was not modulated by expectations or other contextual effects [55,66], although some previous studies have found modulations with some types of interventions [62,67], sometimes with very small effect size [49].

Conversely, the SIIPS was found to be affected by expectations and related psychological manipulations such as placebo treatment [55], perceived control and conditioned cues [66]. Notably, a study using social distribution cues like the ones we have used here found no effects of the cues on the NPS and SIIPS scores [10].

We computed a dot product based score, the 'pattern response', for each trial, and included the scores for each neuromarker in mixed-effects models identical to the ones used for the behavioral pain ratings. The NPS score was significantly higher for high compared to low intensity painful stimuli ($\beta = 0.143$, $SE = 0.027$, $t_{(2895.21)} = 5.23$, $p < .001$), replicating previous studies. However, it was not significantly affected by the cue mean ($\beta = 0.022$, $SE = 0.030$, $t_{(202.09)} = 0.74$, $p = .462$), variance ($\beta = 0.006$, $SE = 0.027$, $t_{(2895.26)} = 0.24$, $p = .812$), or skewness (positive vs. symmetric: $\beta = 0.017$, $SE = 0.038$, $t_{(2895.6)} = 0.45$, $p = .653$; symmetric vs. negative: $\beta = 0.047$, $SE = 0.039$, $t_{(2894.92)} = 1.21$, $p = .225$). The cue mean x cue variance interaction was also not significant ($\beta = 0.006$, $SE = 0.027$, $t_{(2904.36)} = 0.21$, $p = .836$). Thus, the NPS response depends on the noxious input, and is not modulated by the cues (Figure 5B).

Conversely, the SIIPS score assimilated towards the cue mean ($\beta = 0.066$, $SE = 0.028$, $t_{(2936.51)} = 2.33$, $p = .020$; (Figure 5B)), but was not significantly affected by the stimulus intensity ($\beta = -0.017$, $SE = 0.028$, $t_{(2936.19)} = -0.59$, $p = .552$), cue variance ($\beta = 0.016$, $SE = 0.028$, $t_{(2937.62)} = 0.55$, $p = .586$), or cue skewness (positive vs. symmetric: $\beta = -0.012$, $SE = 0.040$, $t_{(2937.06)} = -0.31$, $p = .757$; symmetric vs. negative: $\beta = -0.011$, $SE = 0.040$, $t_{(2936.81)} = -0.27$, $p = .785$). The cue mean x cue variance interaction was not significant ($\beta = -0.007$, $SE = 0.028$, $t_{(2936.44)} = -0.24$, $p = .814$). Importantly, the NPS and SIIPS are pain neuromarkers, and should not respond to neutral visual stimuli. Indeed, when testing the NPS and SIIPS scores during perception of visual stimuli, there were no significant effects of stimulus intensity or cues (all $ps \geq .094$; Supplementary Table 2).

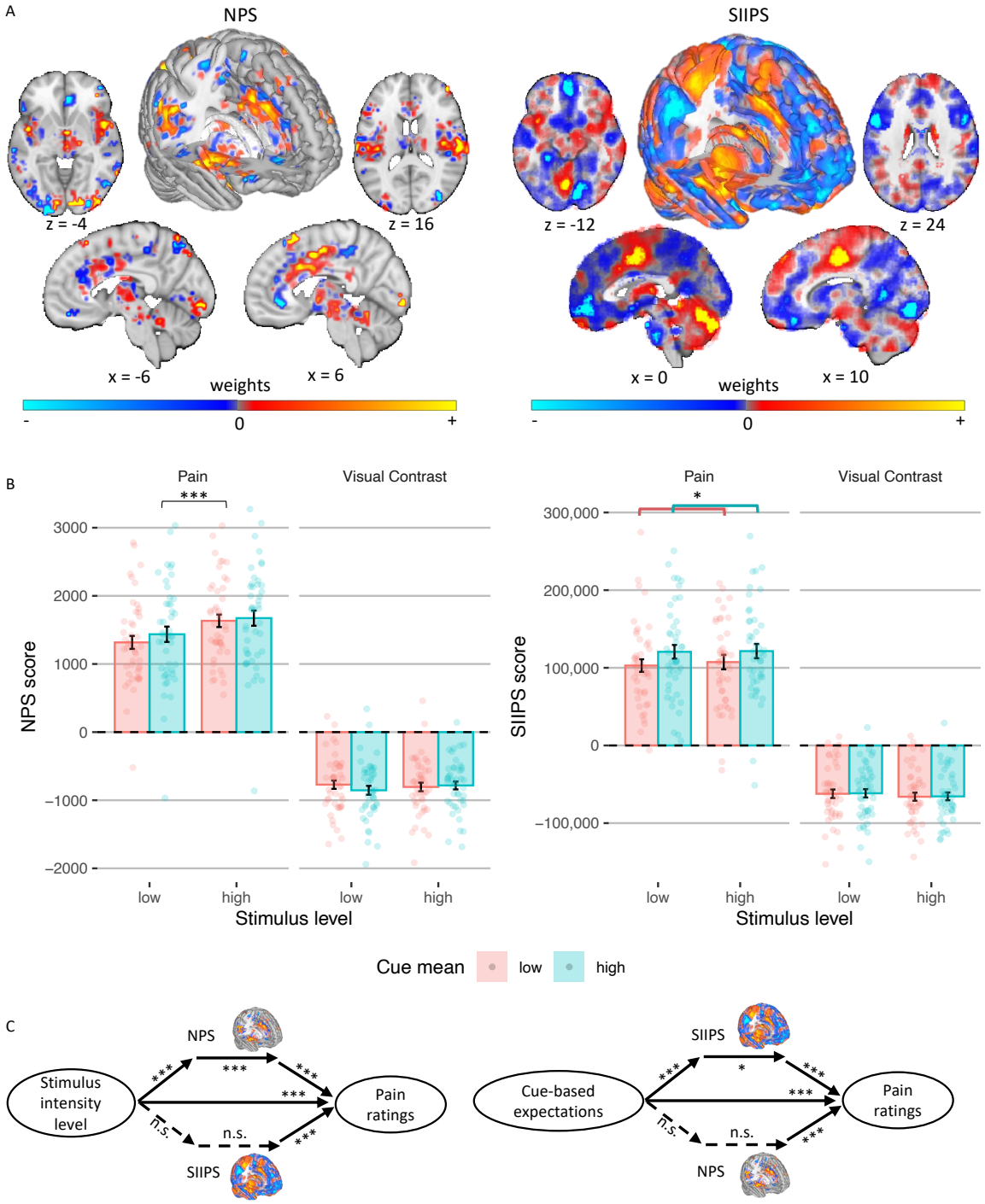

Figure 5. Neuromarker results. (**A**) The NPS and SIIPS neuromarkers. (**B**) NPS (left) and SIIPS (right) score as a function of the stimulus intensity (x axis), cue mean (color) and modality (column). Bars represent averages across participants, error bars represent the standard error of the mean across participants, and points represent single participants. (**C**) Multilevel mediation analysis with pain neuromarkers. Solid lines represent significant effects and dashed lines represent non-significant effects. Asterisks represent the level of significance (* $p < .05$, *** $p < .001$).

Multilevel mediation analysis. We used mediation analysis to test whether the NPS and / or SIIPS formally mediate the effect of the cue-based expectations and/or stimulus intensity on trial-by-trial pain reports (Figure 5C). Trial-by-trial expectancy scores were based on the computational model (see "Computational model: weighting of cue values" above). Expectancy models controlled for stimulus intensity as a covariate, and vice versa.

The NPS partially mediated the effect of stimulus intensity level on pain ratings (*path ab* stimulus intensity level → NPS score → pain rating: $\beta = 0.02$, $SE = 0.00$, $z = 3.68$, $p < .001$), controlling for cue-based expectations. Higher stimulus intensities led to higher NPS scores (*path a*, $\beta = 0.11$, $SE = 0.01$, $z = 4.00$, $p < .001$), and higher NPS scores predicted greater trial-by-trial pain (*path b,* $\beta = 0.28$, $SE = 0.02$, $z = 3.85$, $p < .001$). However, the NPS did not mediate the effect of the cue-based expectations on pain ratings (*path ab* cue-based expectation → NPS score → pain rating: $\beta = 0.00$, $SE = 0.00$, $z = 1.42$, $p = .154$), controlling for stimulus intensity level, since higher cue-based expectations did not lead to higher NPS scores (*path a*, $\beta = 0.02$, $SE = 0.02$, $z = 1.24$, $p = .216$).

Conversely, the SIIPS partially mediated the effect of the cue-based expectation on pain ratings (*path ab* cue-based expectation → SIIPS score → pain rating: $\beta = 0.003$, $SE = 0.001$, $z = 2.45$, $p = .014$), controlling for stimulus intensity level. Higher cue-based expectations led to higher SIIPS scores (*path a,* $\beta = 0.06$, $SE = 0.01$, $z = 3.88$, $p < .001$), and higher SIIPS scores predicted greater trial-by-trial pain (*path b* SIIPS score → pain rating: $\beta = 0.15$, $SE = 0.03$, $z = 3.82$, $p < .001$). The SIIPS did not mediate the effect of the stimulus intensity level on pain ratings (*path ab* stimulus intensity level → SIIPS score → pain rating: $\beta = 0.00$, $SE = 0.00$, $z = 1.37$, $p = .171$), controlling for cue-based expectations, since stimulus intensity was not associated with SIIPS scores (*path a*, $\beta = 0.02$, $SE = 0.01$, $z = 1.23$, $p = .219$).

As expected, neither neuromarker mediated the effect of the stimulus intensity level or the effect of the cue-based expectation on the contrast rating of visual stimuli. Overall, the NPS score was only affected by the heat intensity and formally partially mediated the effect of the stimulus intensity on pain ratings, while the SIIPS score assimilated to the cue mean and partially mediated the effect of the cue-based expectations on pain ratings. Other properties of the cue, including the cue variance, skewness, and the interaction between the cue mean and cue variance, did not affect

either neuromarker. These results indicate that the cues did not affect pain via changes in early nociceptive pain processing, but rather via systems associated with endogenous contributions to pain perception [55].

Effects on ROIs related to early neural perceptual processing. To complement neuromarker analyses, which capture activity in distributed systems, we tested whether the cues affected activity in several a priori ROIs related to pain and visual perception (Figure 6; for all regions see Supplementary Table 1). We first focused on regions associated with early perceptual representations (for full statistics see Supplementary Table 3 and Supplementary Table 4). For nociception, we focused on the spinothalamic tract, including ventral posterior (VPL/VPM) thalamus and dorsal posterior insula (dpIns). Activity in these regions was larger for more intense heat stimuli (all ps $\leq .003$), but was not affected by the cue mean, cue variance, cue skewness, or cue mean x cue variance interaction (all ps ≥ 0.141). For early visual perception, we focused on the lateral geniculate nucleus (LGN) and primary and secondary visual cortex (V1 and V2). Activity was higher for higher visual contrast in the right V1 ($p = .041$) and left V2 ($p = .028$), but not in the LGN (right $p = .438$; left $p = .332$), left V1 ($p = .067$) and right V2 ($p = .058$). Like early nociceptive pain perception, early visual perception was not affected by the cues (negative vs. symmetric cues in right V2 $p = .072$ and left V2 $p = .056$; all other ps > 0.153). Thus, in sum, most of these areas showed stimulus intensity effects, but none were influenced by the cues.

Effects on ROIs related to neural perceptual processing. We then tested cue effects on regions associated with higher-level perceptual processing and affect (Figure 6; see Supplementary Tables 5 and 6 for full statistics). For pain, these included the periaqueductal gray (PAG), anterior midcingulate cortex (aMCC), and medial thalamus. For visual perception they included V3, V4 and V5 (MT). Activity in all pain processing regions was again higher for higher noxious stimulus intensity (all ps $\leq .001$), but only the PAG was sensitive to predictive cues: PAG activity was higher following low- vs. high-mean cues ($p = .031$), consistent with aversive PE-like responses found in the PAG in previous studies [68,69]. In the visual perception task, activity in visual regions was only higher for higher visual contrast in V3 (right $p = .046$, left $p = .017$; all other ps $\geq .193$). While the cue mean, cue variance, and the interaction between them was not significant for any of these visual regions (all ps $\geq .106$), the cues' skewness did affect activity: Activity was lower following negatively skewed compared to symmetric cues in bilateral V3 (right, $p = .009$; left, $p =$

.032), bilateral V4 (right, $p = .010$; left, $p = .045$), and left V5 ($p = .027$). Activity was not different following positively skewed compared to symmetric cues in all regions (all $ps \geq .111$). Overall, the results validate the PAG's role in PEs, but provide no evidence for assimilation to cue value or encoding of cue precision in pain, and only weak evidence for assimilation to extreme low-value cues in visual areas.

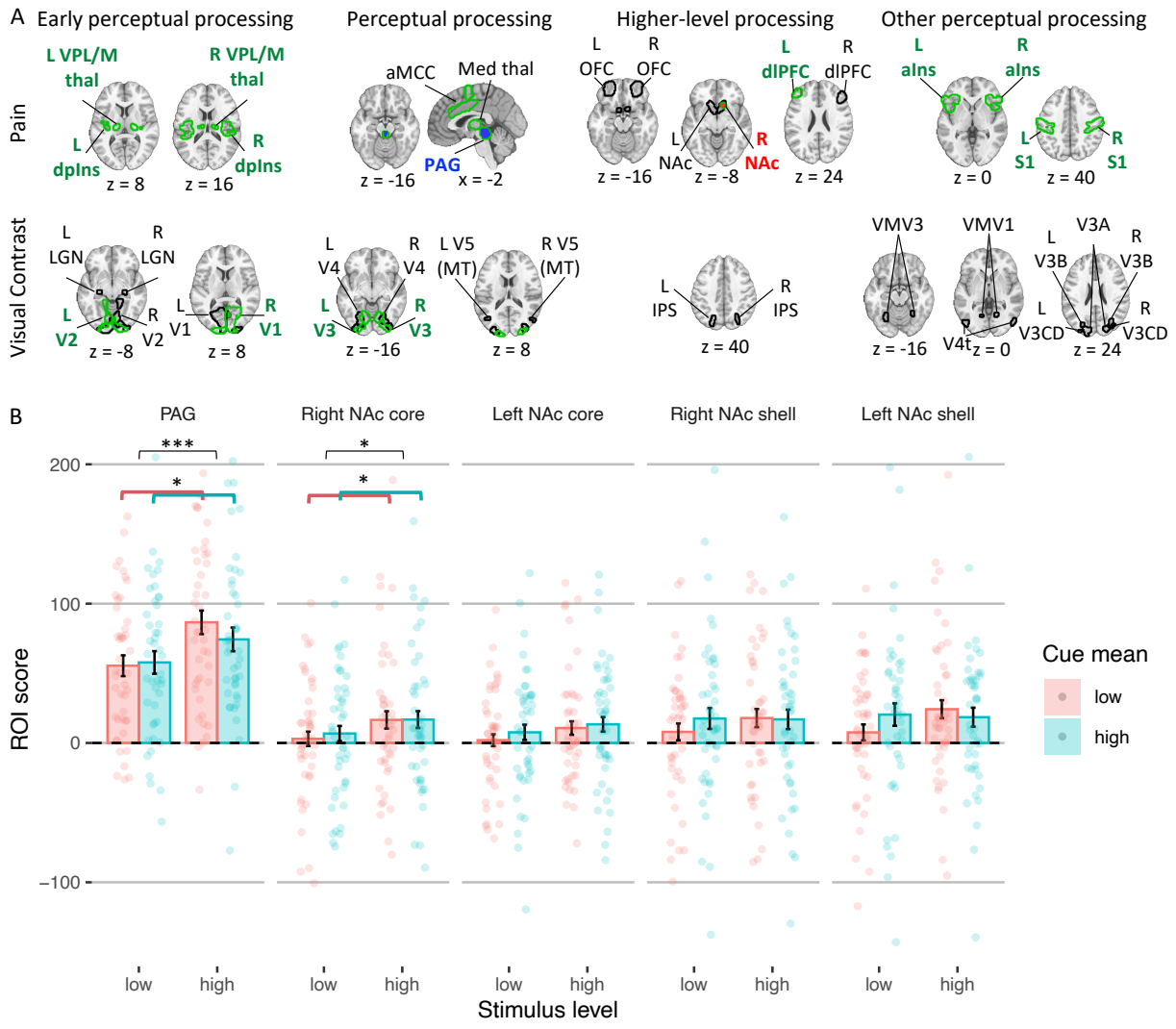

Figure 6. ROI results. (**A**) ROIs are shown with a contour for each modality (rows) and processing stage (columns). Regions with higher activity for more intense stimuli are presented with a green contour. Regions with a significant cue mean effect are presented in red (higher activity for higher cue mean) or blue (higher activity for lower cue mean). (**B**) The ROI score in the two regions with significant cue mean effect during pain perception (including other parts of the NAc) as a function of the stimulus intensity level (x axis) and cue mean (color). Bars represent averages across participants, error bars represent standard error of the mean across participants, and points represent single participants. Asterisks represent the level of significance (* $p < .05$, *** $p < .001$). Abbreviations: aIns = anterior insula; aMCC = anterior

midcingulate cortex; dlPFC = dorsolateral prefrontal cortex; dpIns = dorsal posterior insula; L = left; Med = medial; NAc = nucleus accumbens; OFC = orbitofrontal cortex; PAG = periaqueductal gray; R = right; thal = thalamus.

Effects on ROIs related to higher-level processing. Next, we tested regions associated with higher-level affective and cognitive processing of noxious and visual stimuli, including the nucleus accumbens (NAc; shell-like and core-like parts), dorsolateral prefrontal cortex (dlPFC) and mid-lateral orbitofrontal cortex (OFC) for pain, and the intraparietal sulcus (IPS) for visual perception (Figure 6; see Supplementary Tables 7 and 8 for full statistics). Activity was higher for more intense heat stimuli in the right NAc (core-like part; $p = .017$) and left dlPFC ($p = .001$). The cues only affected activity in the NAc (core-like part; all other ps $\geq .070$): Activity in the right NAc was higher following cues with a higher mean ($p = .018$) and lower variance (i.e., more certain; $p = .011$), and activity in the left NAc was higher for low-variance (more precise) cues ($p = .001$) and showed a cue mean *x* cue variance interaction ($p = .015$), such that cue mean effects were smaller for more precise cues. These findings were not in line with previous predictive coding findings [25,70] (see Discussion). In visual perception, activity in the IPS was not affected by the stimulus intensity or the cues (cue mean effect: $p = .066$ in the left and $p = .074$ in the right IPS; cue mean x cue variance interaction in the right IPS $p = .064$; all other ps $\geq .216$).

Effects on other perceptual processing regions. Finally, we performed an exploratory analysis testing a larger set of regions, including anterior insula (aIns) and primary somatosensory cortex (S1, mostly the hand area) for pain processing, and V3A, V3B, V3CD, V4t, VMV1, VMV2, and VMV3 for visual processing (Figure 6; see Supplementary Tables 9 and 10 for full statistics). Activity during pain perception was higher for higher stimulus intensity in the aIns (right $p = .007$; left $p = .001$) and S1 (both $p < .001$), but the cues did not affect their activity (negatively skewed vs. symmetric cues in the right aIns $p = .075$, all other ps ≥ 0.225). Interestingly, activity was higher (less negative) with more intense heat in several visual regions, possibly because noxious heat stimuli produce diffuse effects on neuromodulatory systems, but none showed cue effects (see Supplementary Results). In response to visual stimuli, none of the additional regions were affected by the stimulus intensity or cues, except for V3A, where activity was lower following negatively skewed compared to symmetric cues (right $p = .021$, left $p = .010$).

Overall (see Supplementary Figure 1 and Supplementary Figure 2 for all effects across all regions), strong effects of stimulus intensity in pain and moderate effects in vision validated the sensitivity

of ROIs to stimulation, but cue effects on stimulus-evoked activity were limited. In pain, we found aversive PE-like responses in the PAG and, in NAc, assimilation to cues and effects of cue uncertainty. However, the latter effects were not in line with previous theoretical predictions and findings [25,70–72]. In vision, we found limited assimilation towards extreme low-value cues in some visual areas. Finally, several nociceptive regions, as well as the NPS, assimilated to the cue mean during the anticipation period, but were not affected by the cue's precision (see Supplementary Results).

Discussion

Current models of perception emphasize the importance of predictive processes in constructing perceptual experience across modalities. Perception has been shown to assimilate towards expected values in different modalities, such as pain [7,8,10–12], vision [5,13,14], audition [73–75], taste and olfaction [76], and interoceptive experiences like itch [77] and nausea [78]. Consistent with these findings, in the current study both reported expectations and perceptions showed strong assimilation towards predicted values (cue mean) in both pain and visual intensity judgments. Furthermore, this assimilation persisted throughout the experiment although the cues were not reinforced, and was highly correlated across modalities, suggesting domain-general susceptibility to cues and/or learning. While several brain regions responded more to more intense stimuli, only neural activity related to higher-level pain processing was modulated by the cue mean. Behaviorally, in line with Bayesian predictive coding accounts [5,6,22], we found that overall the effect of the cue mean on perception was stronger when cue precision was higher. However, ratings were also overall higher following less precise cues, and no brain regions showed activation patterns consistent with these effects (but see below). Finally, we found that when generating expectations, people overweight extreme values across modalities, and also smaller values specifically in pain.

Our findings are mostly consistent with Bayesian predictive processing accounts, but provide new evidence addressing several open questions and potentially accounting for several previous contradicting findings. First, while the prediction regarding assimilation to expected values is straightforward at the behavioral level, where and how the brain encodes this information is much less clear. One hypothesis is that brain representations related to perceptual experience should assimilate towards predicted values. Here, early nociceptive and visual regions – and a

neuromarker for nociceptive pain, the NPS – did not show evidence for assimilation towards predicted values during perception, nor did higher-level perceptual regions such as the aMCC and aIns in pain or V3, V4 and V5 in visual perception. Only the right NAc and SIIPS, a distributed neuromarker for pain related to endogenous sources (including signal in dmPFC, aIns, vmPFC, and other regions), showed significant assimilation to predicted values. These results suggest that early perceptual processes are relatively shielded from influences of conceptually driven predictions, and the strong effects on perception are driven by higher-level evaluative processes, in line with psychological accounts questioning early influences of context information on perception [51] and recent findings in the context of placebo analgesia [55]. Such effects might also depend on the type of cues used. Indeed, a previous study using cues similar to the ones we have used here, has found that frontoparietal areas involved in high-level construction of perception and value (e.g., dlPFC, OFC and IPS) mediated cue effects on pain, whereas classically conditioned cue effects were mostly mediated by different systems [10].

Predictive processing theories also emphasize coding of PEs ('predictive coding' [6,79,80]), a contrast with predictions that provide efficient representations of salient changes in the environment and drive the updating of internal models (learning) [24,71,81]. Which areas show brain responses that assimilate to predictions or contrast with them (encode PE) is currently an active area of investigation. A working hypothesis is that early sensory areas encode sensory PEs, as they are relatively distal from internal models and shielded from their effects, whereas higher-level perceptual areas encode posterior perceptions, which represent stimuli but assimilate to predicted values. This may be particularly true when internal predictive models are conceptual, including the kinds of non-reinforced cues about others' experience that we studied here. Here, PAG activity was higher following low vs. high cue mean, consistent with pain-related aversive PE that was found in the PAG in previous studies [68,69]. Together with the assimilation towards predicted values in higher-level systems, our results largely support this working hypothesis, although we do not directly test encoding of different types of PEs [80].

Bayesian accounts of brain function also make specific predictions about the precision of expectations. More certain (precise) cues should have stronger effects on perception [5,6,22]. Some previous studies have provided support for this hypothesis by using the precision of stimulus history as a proxy for predictive precision [25,27]. The kinds of cues with distributions we used here

offer particular advantages in studying cue precision, as the cue mean, variance (i.e., inverse precision) and other properties (e.g., extreme values) can be independently experimentally manipulated across cues. Studies using this type of cues have found results that contradict predictive processing accounts by finding null effects of cue precision [30] or even direct effects of predictive uncertainty on increased pain perception [7]. In the current study, cue precision effects on perceptual ratings supported Bayesian predictive processing accounts (by showing a cue mean x variance interaction; although the effect was not significant when tested only in pain). In addition, more uncertain cues led to higher ratings, as expected by the uncertainty aversiveness account, but this effect was again significant in visual perception but not pain, and thus does not support the interpretation of Yoshida et al. [7], who suggested that uncertainty is aversive in the context of pain.

Several studies have recently explored the neural correlates of expectations' precision. Predictive processing accounts predict that perceptual activity will be higher following less precise cues, because of stronger reliance on incoming sensory information. Indeed, studies have shown decreased PAG fMRI activity [25] and early EEG responses [70] for more precise expectations. Here, perceptual responses were not affected by the cue precision in both modalities, including in the PAG. The only region that was affected by the cue precision was the NAc, where activity was higher following more (rather than less) precise cues during pain perception. While this effect was in opposite direction from the effects previously shown in other (earlier) regions, it could be consistent with predictive processing, since activity in the NAc might represent the priors (expectations) and thus is expected to be stronger when the priors are more precise (and also when they are stronger, and indeed NAc activity assimilated to the cue mean).

Our design also allowed us to study effects of extreme cue values, and test how participants weight predictions of upcoming pain and visual contrast across the distribution from low to high values, which has been studied in the context of magnitude judgments [42,43] but not, to our knowledge, in pain. If participants over-weight extreme high-pain values – e.g., attend most to the most threatening potential values – that might explain why Yoshida et al. found increased pain with high-variance cues [7] while other studies have not found a main effect of uncertainty on pain [30,35]. Here, we found that perceptual ratings were drawn towards larger extreme values, but this effect, like the effects of the cue variance, was significant mostly in visual perception and not in pain perception.

Since noxious stimuli are considered to be more ambiguous and subjective compared to visual stimuli, we expected reduced cue effects on visual perception. Indeed, computational modeling indicated that the cues were weighted more strongly in pain compared to visual perception. On the other hand, the variance and skewness of the cues mostly affected visual and not pain perception. These findings suggest that overall expectations affect pain perception more, but visual perception is more sensitive to the precision of the expectations. Finally, the persistent effects of the non-reinforced cues in both pain and visual perception might represent modulation of early perceptual processes, modulation of perceptual decision-making (higher-level affective and cognitive processes), or a post-experience report bias (i.e., demand characteristics [82], or conformity to alleged ratings of other participants [83]). Our neural results suggest that cues affect perceptual decision-making, since activity in regions related to early perceptual processing was not affected, while neural activity related to higher-level processing was affected by the cues, at least in pain. Moreover, neural effects were different between the two modalities, indicating that expectation effects are modality-specific rather than modality-general, even when they operate on higher-level processes.

Beyond the effect of the cues on perception, we also studied how expectations are generated from multiple values, and anticipatory neural responses. Reported expectations assimilated towards mean values. Anticipatory responses in several pain regions, including the insula, aMCC, PAG, and even the NPS, were higher for high vs. low cue mean, while the opposite direction was found on visual trials, with lower anticipatory activity for high vs. low cue mean in several visual regions (Supplementary Results). Beyond the assimilation to the mean value, reported expectations were also biased towards extreme values in both modalities, and specifically smaller values in pain. Such effects might depend on the characteristics of the sample. The current sample consisted of healthy young adults, who may have been looking for safety signals as part of an optimism bias or may have viewed themselves as less sensitive to pain compared to others (and thus trusted lower ratings more). Putatively, different populations, such as chronic pain patients, might instead look for risk signals or view themselves as more sensitive to pain, and thus overweight larger values. Perhaps surprisingly, the tendency to overweight smaller values when forming expectations did not correlate with personality or state measures such as fear of pain, pain catastrophizing, or state anxiety. However, a growing literature suggests that task-based and self-report measures are often unrelated [84,85] and assess different constructs over different contexts and time scales [86,87].

Several limitations should be considered in the context of the current findings. First, the effects of the cue variance and skewness that were found were almost all relatively weak, and the main driver of cue effects on perceptual processing was the cue mean. Second, the inclusion of both modalities in the same experiment with interleaved blocks may have yielded cross-modality dependency that could have driven some of the results, such as the correlation between the effect of the cue mean on pain and visual ratings. Third, we did not directly compare the effects between pain and visual perception, since the scales are not directly comparable between modalities (e.g., a 10-point or a 20% increase in visual contrast rating is not necessarily perceptually equivalent to the same increase in pain rating).

Taken together, our findings suggest that perception is more complex than the recent Bayesian-driven focus on the mean and uncertainty of contextual information. More specifically, they show that extreme values have an important role in how people integrate information into expectations that later affect perception. Furthermore, these findings suggest that some aspects of expectation formation and their effect on subsequent perception are modality-general (e.g., the assimilation towards the cue mean and the importance of extreme values), while others are modality-dependent (e.g., the overweighting of smaller vs. larger values and the weight given to contextual information). Better understanding of these processes and differences between sub-populations and modalities would advance our knowledge of how people form expectations, how these expectations affect perception, and how such processes could be leveraged to improve well-being and clinical care.

Methods

Participants

Forty-five healthy participants (25 females; age range 18-42, mean 24.1 years) completed the study. Five additional participants were excluded because they did not complete the experiment or reported impaired vision or recent substance abuse. Participants reported no history of neurological, psychiatric, dermatologic conditions, and had not taken any medication during the 48 hours period prior to their participation. Participants reporting acute and chronic pain conditions in an initial online screening were excluded from participation. We recruited participants from the University of Colorado Boulder and local community through flyers and online ads. The

Institutional Review Board of the University of Colorado Boulder approved the protocol and participants provided informed consent before the beginning of the experiment.

Procedure Overview

Participants completed three different tasks and a set of questionnaires. First, the stimulus-response task served to estimate the stimulus-response functions for heat pain stimuli of different temperatures and flickering checkerboards of different visual contrasts. Second, in the expectation task, participants rated their expectations about heat pain and visual contrast intensities based on the cues provided in each trial without any actual stimulation. Third, in the cued-perception task, participants rated the perceived painfulness of noxious stimuli and contrask of visual stimuli that were preceded by the presentation of cues.

In session 1, the stimulus-response and expectation tasks were completed outside the MRI scanner in a behavioral laboratory. In session 2 (on average 4.4 days after session 1, range 1 - 11 days), participants first completed a battery of questionnaires on a computer, followed by a brief practice of the cued-perception task outside the scanner. Participants then moved to the MR scanner where they completed another brief practice inside the scanner to get accustomed to the trackball and the MR environment. Following a structural MRI scan, they completed the cued-perception task while their brain activity was measured with fMRI. After the cued-perception task, a functional localizer with different visual checkerboard contrasts was presented to the participants. Finally, participants completed a debriefing questionnaire outside the scanner.

Stimulus-response task

In the first task, topical heat stimuli of five different temperatures and flickering checkerboards of five different luminance contrasts were presented to participants. After each trial, participants rated the perceived painfulness of the heat or luminance contrast of the checkerboard. The task was split into two blocks, one pain block and one vision block. In each block, 25 stimuli were presented in randomized order for a total of 50 stimuli.

Temperatures in the heat block ranged from 45-49°C, in steps of 1°C. Each temperature was used five times and each stimulation lasted for two seconds (including ramp up and down from a 32°C baseline). After a variable delay of 5 – 6 seconds, participants rated the perceived heat intensity on

a computerized visual analogue scale (VAS) by moving a vertical cursor bar on the VAS. The VAS was anchored at "no pain at all" and "worst pain imaginable". Participants were instructed to rate any heat stimulus that was noticed but not painful at the low extreme and that "worst pain imaginable" referred to the context of this experiment. They were further instructed to rate the maximum only in the case that they would have lifted the thermode to stop the experiment, which did not happen. After an inter-trial-interval (ITI) of 2 – 5 seconds, the next trial started. Before the task began, participants experienced two heat stimuli of 47°C without rating, to get familiar with the heat stimulation and reduce potential anxiety. Ratings were converted to a range between 0 - 100 in all tasks and conditions.

Black-and-white radial checkerboards were presented in block 2 at 5%, 27.5%, 50%, 72.5%, and 95% luminance contrast. Checkerboards were presented for two seconds in each trial and the contrast of each checkerboard reversed at a frequency of 8 Hz to increase responses in visual brain regions. Checkerboards covered 12° visual angle in both the behavioral and the fMRI experiment and both screens were calibrated to display the same luminance level and contrast. After each stimulus, participants rated the perceived contrast on a VAS anchored "no contrast at all" and "strongest contrast". Similar to the pain block, an ITI of 2 – 5 sec separated two consecutive trials.

Expectation task

In the expectation task, participants saw different distributions of intensity ratings on a computer screen and reported their expected intensity of either heat pain or luminance contrast based on these ratings. Participants were informed that the rating distributions represented the ratings of other people for heat and checkerboard stimuli similar to those they just experienced in the stimulus-response task. The ratings were marked as vertical bars on visual analogues scales as used in the stimulus-response task (see Figure 1). A set of 10 ratings was presented on a single VAS in each trial for 1.5 seconds. After a brief delay of 1.75 seconds, participants rated their expected pain intensity or contrast intensity on the same VAS as in the stimulus-response task.

The distribution of ratings shown to the participants were determined by factorial combinations of their different distribution means (five levels, $M \in [30, 40, 50, 60, 70]$), standard deviations (two levels, $SD \in [5, 12.5]$), and skewness (three levels: negative, positive, or symmetric). Symmetric distributions were drawn from a normal distribution and skewed distributions were drawn from a

log-normal distribution. Skewness was < -0.3 for negatively skewed, > 0.3 for positively skewed, and between -0.035 to 0.035 for symmetric distributions. Here, only 9 instead of 10 elements were sampled from the log-normal distribution. A 10th element was added between 2.0 – 2.5 standard deviations above or below the mean, respectively, to ensure that each skewed distribution included at least one extreme rating. All rating distributions were re-sampled if necessary to ensure that the properties of the distribution matched the specified mean, standard deviation, and skewness, as well as the independence of the factors across trials.

Participants completed a total of 360 trials in this task split into six blocks. Participants rated heat pain expectations in three consecutive blocks and contrast intensity in the other three consecutive blocks, with the order counterbalanced across participants (three pain and then three visual or three visual and then three pain blocks). The combination of the four factors (modality, mean, standard deviation, and skewness) resulted in a total of 60 combinations. Each combination was repeated six times, once per block. The order of trials was randomized for each participant within each block.

Cued-perception task

The cued-perception task combined the two previous tasks into a single task performed inside the MRI scanner. In each trial, participants were cued with rating distributions (as in the expectation task) for 1.5 seconds before being presented with either cutaneous heat or a flickering checkerboard for two seconds (as in the stimulus-response task). Cues and stimulation periods were separated by a brief interval of 2.5 - 5.5 seconds. Participants rated the perceived intensity of the heat or luminance contrast after another brief interval of 3 - 6 seconds. Participants had 4.5 seconds to rate the intensity using an MR compatible trackball. Trials were separated by an ITI of 3 – 6.5 seconds.

In this task, stimulation modality (heat vs. visual) and two levels of stimulation intensity were combined with different rating cue distributions similar to those used in the expectation task. The rating cues were drawn from distributions with two means ($M \in [30, 70]$), two standard deviations ($SD \in [5, 12.5]$), and three levels of skewness (negative skew, symmetric, positive skew). Ten ratings were presented in each trial on a VAS as described for the expectation task. The factorial combination of stimulation modality, stimulation intensity, cue distribution mean, cue distribution

standard deviation, and cue distribution skew resulted in a total of 48 combinations. Each combination was presented three times to each participant resulting in a total of 144 trials split into six blocks. Each block constituted a separate fMRI recording run and included 24 trials split into two mini-blocks of 12 trials each, in which only one modality was presented. The order of modality mini-blocks and the order of trials within modality was randomized for each participant. Skin conductance was recorded during the cued-perception task. Following the cued-perception task, participants completed a visual functional localizer task, in which they were presented with a visual checkerboard with varying contrasts. Data from this task were not used in any of the analyses reported in the current paper.

Apparatus and recordings

Heat stimulation. An fMRI compatible Peltier thermode (1.5 × 1.5 cm surface, PATHWAY ATS; Medoc, Inc, Israel) delivered heat to the left volar forearm of the participant in the stimulus-response task and the cued-perception task. The total stimulus duration was two seconds including ramp up and down from a 32°C baseline with extremely fast ramps (70°C/second up and 40°C/second down).

Visual stimulation. Radial checkerboards with a diameter of 12° visual angle flickered at a rate of 8 Hz on a 50% gray background. Screen luminance was calibrated using a Minolta LS-100 luminance meter. Stimulus presentation, thermode control, and response logging were implemented using the Psychophysics Toolbox (PTB-3, http://psychtoolbox.org/) [88].

Behavioral data Analysis

Analyses were performed with R version 4.3.1 (R studio version 2023.09.0+463). For reproducibility, we used the *checkpoint* package, which installs the R packages included in the code as they were on a specific date. We set the date to April 1, 2024. 211 out of 6480 trials in the cued-perception task were excluded due to technical issues with the pain device, rating device, or MRI scanner. Additional 234 trials were excluded because the ratings were too fast to represent deliberate ratings (response time < 0.2 second) or were not completed during the 4.5 seconds long rating period (response time > 4.5 seconds).

Linear mixed-effects models were fit to the perception (stimulus-response task and cued-perception task) and the expectation (expectation task) ratings with R's lmer function, with the packages "lme4" [89] and "lmerTest" [90]. All statistical tests were two-sided. In the stimulus-response task, regressors coding modality (pain vs. vision), stimulus intensity level, and the interaction between these two variables were included in the model as fixed effects. We also fitted two additional models, one for each modality (i.e., one with pain trials only and one with visual trials only), with the stimulus intensity level as a regressor. In the expectation task, included regressors were modality, cue mean, cue variance level, and cue skewness level, with all their interactions. Again, we also fitted an additional model for each modality separately, with the same regressors (except for modality and its interactions). In the cued-perception task, we included the modality, stimulus intensity level, cue mean level, cue variance level, and cue skewness level as regressors (along with their interactions). In all tasks, when significant interaction effects were found, we tested the related simple effects. All numeric variables (ratings, intensity level for the stimulus-response task, and cue mean for the stimulus-response and expectation task) were z-scored. Binary variables (modality, cue intensity level, cue variance level, and cue mean level in the cued-perception task) were modeled with one regressor, coded as 1 (pain, or high intensity level / cue mean / cue variance level) and -1 (vision, or low intensity level / cue mean / cue variance level). The cue skewness level was modeled with two regressors using the symmetric condition as the reference.

Moreover, in all models, participants were modeled as random effects. In each model, we started with a maximal random effects structure, modeling all random effects (intercept and slopes) and their correlations [91]. In case the model did not converge properly, we simplified the maximal model by first removing the random correlations and then reducing the random terms that indicated model converges issues (i.e., correlations of 1, or random variance of 0). Using these criteria preserves type I error while potentially increasing power when random effects estimates are near the boundary values [92].

Computational modeling

Expectation data. We developed a computational model to test how expectations are generated from the cue data, which consists of 10 values per cue. The model assumes that in each cue, each of these 10 values is weighted based on its relative location in the distribution of the 10 values

(Figure 3; the model was largely inspired by Spitzer et al., 2017 [43]). The model yields a weight for each value, based on a combination of a power term modeling the weighting of inliers vs. outliers and a logistic term modeling the weighting of values that are smaller vs. larger than the mean. First, all 10 values of each cue were rescaled to [0,1] and then demeaned, such that cue values smaller than the mean were negative and cue values larger than the mean were positive. We denote the rescaled and demeaned value X_i (where i ranges from 1 to 10 cue values).

Second, for each X_i, we computed a "power term" weight with the following equation:

(1) $$Wk_i = \frac{sign(X_i) * |X_i|^k}{X_i}$$

Where Wk_i is the power term weight of X_i, and $k \in (0, 1000]$ is a free parameter. When $k < 1$ inliers are over-weighted, when $k = 1$ outliers and inliers are equally weighted, and when $k > 1$ outliers are over-weighted. Wk_i values for each cue where then normalized to [0,1] by dividing each Wk_i by the sum of all Wk weights for each cue $\sum_{i=1}^{10} Wk_i$.

Third, for each X_i, we computed a "logistic" weight using the following equation:

(2) $$Wb_i = \frac{1}{1+e^{(-b*X_i)}}$$

Where Wb_i is the logistic weight of X_i, and $b \in [-1000, 1000]$ is a free parameter. When $b < 0$ values that are smaller than the mean are over-weighted, when $b = 0$ all values are equally weighted, and when $b > 0$ values that are larger than the mean are over-weighted. Wb_i values are mathematically bounded between [0, 1].

Fourth, the two weights were combined, and normalized to the range [0,1], such that the weight of each X_i was:

(3) $$W_i = \frac{Wk_i + Wb_i}{\sum_{i=1}^{10}(Wk_i + Wb_i)}$$

Finally, the expectation based on each cue was computed as the sum of each value V_i multiplied by its weight W_i:

(4) $$Expectation = \sum_{i=1}^{10}(V_i * W_i)$$

Thus, the model computes an expectation value for each cue. The model was fitted to all trials (cues) of the expectation task of each participant. The free parameters k and b were optimized per participant and modality, based on ordinary least squares (OLS), with Matlab version 2022a *lsqcurvefit* function. We then tested whether the optimized k was significantly different from 1 and whether the optimized b was significantly different from 0 at the group level, separately in each modality, with two-sided Wilcoxon signed rank tests. We also tested the correlation between the optimized k for pain and for vision across participants, and the same for the optimized b, with a two-sided Spearman correlation test.

Perception data. We developed five competing nested models for the cued-perception task. Models were fitted and optimized at the participant level based on OLS between the model's predicted rating and the empirical ratings provided by the participants. Similarly to the expectation data model fitting, we used Matlab's *lsqcurvefit* function. Then, we performed model comparison at the participant level with F tests, to test, for each participant, whether each model improves the fit compared to its nested, simpler model. To make inferences regarding the best fitting model at the group level, we performed F tests based on the mean residual sum of squares across participants, and also computed the Akaike Information Criterion (AIC) for each of the five models.

Model 1: Baseline Model. This model assumes participants are not affected by the cues, and their rating in each trial (t) depends only on the intensity of the stimulus:

$$\text{rating}(t) = \text{intensity}(t) * s \tag{5}$$

The intensity is based on the average rating of each participant for the given stimulus modality and intensity from the stimulus-response task. $s \in [0, 5]$ is a free parameter that is used for scaling of participants' ratings for each intensity from the stimulus-response task to the cued-perception task, which happened on a different day and in a different context (inside the MRI scanner). The Baseline Model includes two such scaling factors: s_p scales the pain stimuli, and s_v scales the visual stimuli. These two free parameters are included in all models.

Model 2: Expectation Model. This model assumes that in each trial, participants weight the cue and the stimulus to generate their rating. The weighting is determined by an additional free

parameter, $w \in [0, 1]$, that is fixed throughout the task for each participant and is the same for both modalities (thus, the model includes three free parameters):

$$\text{rating}(t) = (1 - w) * \text{intensity}(t) * s + w * \text{expectation}(t) \quad (6)$$

The expectation value in each trial is generated from the cue presented on that trial, with the model that was optimized for each participant based on the expectation task data (see above).

Model 3: Expectation Learning Model. This model adds a reinforcement learning component, such that w is updated based on PEs (the difference between the cue-based expectation and the rating), with learning rate $\alpha \in [-1, 1]$. The rating in each trial is computed with equation 6, as in the Expectation Model, but w is updated in each trial based on the previous trial:

$$\text{PE} = \text{rating}(t) - \text{expectation}(t) \quad (7)$$

$$w(t + 1) = w(t) - \alpha * \text{PE}(t) \quad (8)$$

This model includes four free parameters: The two scaling factors s_p and s_v, the initial weighting factor $w(t = 0)$, and the learning rate α.

Model 4: Expectation Model by Modality. This model is similar to the Expectation Model, beside one difference: the weighting factor, w, is separated to w_p for the pain modality and w_v for the visual modality. Thus, it includes four free parameters.

Model 5: Expectation Learning Model by Modality. This model is similar to the Expectation Learning Model, with two additions: Both the initial weighting factor ($w(t = 0)$) and the learning rate (α) are optimized separately for the pain (w_p and α_p) and visual (w_v and α_v) modalities. Thus, it includes six free parameters.

Neuroimaging

Neuroimaging data acquisition. Data were collected on a 3 Tesla Siemens Trio MRI scanner with a 32 channels head coil at the University of Colorado Boulder Center for Innovation and Creativity. A high-resolution T1-weighted magnetization-prepared rapid gradient echo (MPRAGE) structural scan (0.8×0.8×0.8 mm voxels, TR: 2400 ms, TE 1: 2.07 ms, Flip angle: 8°,

Tl: 1200 ms, FoV Read: 256 mm) was performed on each participant at the beginning of the MR session. We next acquired four images to compute B0-fieldmaps for distortion correction: two images with phase encoding in the anterior-posterior direction and two images with reversed phase encoding (2.7×2.7×2.7 mm voxels, TR: 7.22 s, TE: 73 ms, slices: 48, flip angle: 90°, FoV read: 220 mm). During the cued-perception task, a multiband (eight simultaneous slices) echo-planar imaging (EPI) sequence (2.7×2.7×2.7 mm voxels, TR: 410 ms, TE: 27.2 ms, slices: 48, multiband factor=8, flip angle: 44°, FoV read: 220 mm) was acquired. A single-band reference scan was acquired at the beginning of each run. We acquired 1250 volumes during each run of the cued-perception task and 776 volumes during the visual functional localizer task.

Neuroimaging Data preprocessing. Structural and functional data were preprocessed using fMRIPrep version 20.2.3 (RRID:SCR_016216 [93,94]), which is based on Nipype 1.6.1 (RRID:SCR_002502 [95,96]).

Anatomical data preprocessing. The T1-weighted (T1w) image was corrected for intensity non-uniformity (INU) with N4BiasFieldCorrection [97], distributed with ANTs 2.3.3 (RRID:SCR_004757 [98]), and used as T1w-reference throughout the workflow. The T1w-reference was then skull-stripped with a *Nipype* implementation of the antsBrainExtraction.sh workflow (from ANTs), using OASIS30ANTs as target template. Brain tissue segmentation of cerebrospinal fluid (CSF), white-matter (WM) and gray-matter (GM) was performed on the brain-extracted T1w using fast (FSL 5.0.9, RRID:SCR_002823 [99]). Volume-based spatial normalization to one standard space (MNI152NLin2009cAsym) was performed through nonlinear registration with antsRegistration (ANTs 2.3.3), using brain-extracted versions of both T1w reference and the T1w template. The following template was selected for spatial normalization: ICBM 152 Nonlinear Asymmetrical template version 2009c [[100], RRID:SCR_008796; TemplateFlow ID: MNI152NLin2009cAsym],

Functional data preprocessing. For each of the seven BOLD runs per subject (across all tasks and sessions), the following preprocessing was performed. First, a reference volume and its skull-stripped version were generated from the single-band reference (SBRef). Susceptibility distortion correction (SDC) was omitted. The BOLD reference was then co-registered to the T1w reference using flirt (FSL 5.0.9 [101]) with the boundary-based registration [102] cost-function. Co-registration

was configured with nine degrees of freedom to account for distortions remaining in the BOLD reference. Head-motion parameters with respect to the BOLD reference (transformation matrices, and six corresponding rotation and translation parameters) are estimated before any spatiotemporal filtering using mcflirt (FSL 5.0.9 [103]). First, a reference volume and its skull-stripped version were generated using a custom methodology of fMRIPrep. The BOLD time-series were resampled onto their original, native space by applying the transforms to correct for head-motion. These resampled BOLD time-series will be referred to as preprocessed BOLD in original space, or just preprocessed BOLD. The BOLD time-series were resampled into standard space, generating a preprocessed BOLD run in MNI152NLin2009cAsym space. First, a reference volume and its skull-stripped version were generated using a custom methodology of fMRIPrep. Several confounding time-series were calculated based on the preprocessed BOLD: framewise displacement (FD), DVARS and three region-wise global signals. FD was computed using two formulations following Power (absolute sum of relative motions [104]) and Jenkinson (relative root mean square displacement between affines [103]). FD and DVARS are calculated for each functional run, both using their implementations in Nipype (following the definitions by [104]). All resamplings can be performed with *a single interpolation step* by composing all the pertinent transformations (i.e. head-motion transform matrices, susceptibility distortion correction when available, and co-registrations to anatomical and output spaces). Gridded (volumetric) resamplings were performed using antsApplyTransforms (ANTs), configured with Lanczos interpolation to minimize the smoothing effects of other kernels (Lanczos 1964). Non-gridded (surface) resamplings were performed using mri_vol2surf (FreeSurfer).

Many internal operations of fMRIPrep use Nilearn 0.6.2 ([105], RRID:SCR_001362), mostly within the functional processing workflow. For more details of the pipeline, see the section corresponding to workflows in fMRIPrep's documentation.

Neuroimaging data analysis. fMRI participant-level data processing was carried out using FEAT (FMRI Expert Analysis Tool) v. 6.00, part of FSL (FMRIB's Software Library, www.fmrib.ox.ac.uk/fsl) v. 6.0.4. Data were smoothed with a Gaussian kernel of 5 mm. A 100 hz high pass filter was used during first level analysis. The first level (run level) GLM model included two regressors per trial (48 regressors of interest per run in total): separate regressors for each cue period and for each stimulation period (single trial model, or a "Beta series" [106]). The global CSF

signal and six motion parameters (translation and rotation each in three directions) were included as nuisance regressors. Variance Inflation Factor (VIF) was computed for each trial, and trials with VIF > 5 were excluded. This led to the exclusion of one trial (out of 6058 trials).

Neuromarker and ROI analysis. Group level analysis was performed with Matlab 2022a and 2023a, and CANlab tools (shared via Github at https://canlab.github.io/; also uses SPM12). A score for each neuromarker (NPS and SIIPS) was computed for each trial, once for the cue-evoked period and once for the stimulus-evoked period, based on the dot product between the trial's univariate map (from the singlet trial first-level analysis) and the neuromarker weight map. Similarly, we computed for each trial the averaged activity across voxels of each of the individual a priori ROIs. For each brain measure (neuromarker or ROI), scores that were more than 3.5 SDs away from the mean score (of that same brain measure, period, and modality) were excluded. Overall, this resulted in exclusion of 0.4% of the scores (0.5% of the cue-evoked scores and 0.3% of the stimulus-evoked scores).

In order to allow comparison between the effects on the different brain measures, but keep the between-participants and within-participants effects unchanged, the scores of each brain measure were z-scored across all trials within the scope of the model (combination of modality [pain / visual perception] and period [stimulus-evoked / cue-evoked]) before including them as the dependent variable in the model (i.e., producing standardized beta estimates). Then, the z-scored scores were tested with mixed-effects models, as described above for the expectation / perceptual ratings (models were identical to the models described above, with the neuromarker / ROI score replacing the outcome rating; see Methods section *Behavioral data analysis*).

Multilevel mediation analysis with neuromarkers. We further tested, for each of the two neuromarkers, whether it mediated the effect of the cue-based expectation on the outcome rating, and whether it mediated the effect of the stimulus intensity on the outcome rating, each controlling for the other, for each modality separately. Brain mediation analysis tests whether a variable mediates the relationship between other variables, by identifying three statistical paths [9]. Path *a* captures the effect of the initial variable, usually the experimental manipulation (e.g., the cue-based expectation), on the mediator (e.g., the neuromarker score). Path *b* captures the effect of the mediator on the outcome variable (e.g., the outcome rating). Path *ab* captures the indirect effect of the initial variable on the outcome variable, i.e., the part of the relationship between the initial

variable and the outcome variable that is formally mediated by the mediator. Path *c'* captures the direct effect of the initial variable on the outcome variable, that is not mediated by the mediator.

Here, we tested the effect of the cue-based expectations, or the stimulus intensity level, on the outcome rating, with the neuromarker (NPS / SIIPS) as the mediator. Thus, four mediation models were tested for each modality: (1) Cue-based expectation (the trial-level expectation based on the presented cue and the expectation computational model with each participant's optimized *k* and *b* parameters) → trial-level NPS score → trial-level outcome rating, with trial-level stimulus intensity as a covariate; (2) Trial-level stimulus intensity → trial-level NPS score → trial-level outcome rating, with trial-level cue-based expectation as a covariate; (3) Same as model 1, but with SIIPS instead of NPS; (4) Same as model 2, but with SIIPS instead of NPS. In all four models, the neuromarker score, the cue-based expectation value, and the outcome rating were z-scored across all trials, separately for each modality. Each model was run with CANlab neuroimaging analysis tools' mediation.m function. Mediation was tested with bootstrapping, with 10000 samples [107].

Data and code availability

Processed data and analysis codes are publicly shared on Github: https://github.com/rotemb9/PPRI-paper (release v1.0.0). CANlab neuroimaging analysis tools that were used as part of the analysis are available at https://canlab.github.io/. The raw imaging data will be openly shared upon publication.

Acknowledgements

This study was funded by the National Institute of Mental Health (NIMH; R01MH076136). The funders had no role in study design, data collection and analysis, decision to publish or preparation of the manuscript. Rotem Botvinik-Nezer thanks the Golda Meir Fellowship.

Competing interests

The authors report no competing interests.

References

1. Friston, K. The history of the future of the Bayesian brain. *Neuroimage* **62**, 1230–1233 (2012).
2. Knill, D. C. & Pouget, A. The Bayesian brain: the role of uncertainty in neural coding and computation. *Trends Neurosci.* **27**, 712–719 (2004).
3. Clark, A. Whatever next? Predictive brains, situated agents, and the future of cognitive science. *Behav. Brain Sci.* **36**, 181–204 (2013).
4. Friston, K. The free-energy principle: a unified brain theory? *Nature Reviews Neuroscience* vol. 11 127–138 Preprint at https://doi.org/10.1038/nrn2787 (2010).
5. Summerfield, C. & de Lange, F. P. Expectation in perceptual decision making: neural and computational mechanisms. *Nat. Rev. Neurosci.* **15**, 745–756 (2014).
6. Büchel, C., Geuter, S., Sprenger, C. & Eippert, F. Placebo analgesia: a predictive coding perspective. *Neuron* **81**, 1223–1239 (2014).
7. Yoshida, W., Seymour, B., Koltzenburg, M. & Dolan, R. J. Uncertainty increases pain: Evidence for a novel mechanism of pain modulation involving the periaqueductal gray. *J. Neurosci.* **33**, 5638–5646 (2013).
8. Zhang, L., Wager, T. D. & Koban, L. Social cues influence perception of others' pain. *Eur. J. Pain* (2023) doi:10.1002/ejp.2225.
9. Atlas, L. Y., Bolger, N., Lindquist, M. A. & Wager, T. D. Brain mediators of predictive cue effects on perceived pain. *J. Neurosci.* **30**, 12964–12977 (2010).
10. Koban, L., Jepma, M., López-Solà, M. & Wager, T. D. Different brain networks mediate the effects of social and conditioned expectations on pain. *Nat. Commun.* **10**, 1–13 (2019).
11. Koyama, T., McHaffie, J. G., Laurienti, P. J. & Coghill, R. C. The subjective experience of pain: where expectations become reality. *Proc. Natl. Acad. Sci. U. S. A.* **102**, 12950–12955 (2005).
12. Atlas, L. Y. & Wager, T. D. How expectations shape pain. *Neurosci. Lett.* **520**, 140–148 (2012).
13. Sterzer, P., Frith, C. & Petrovic, P. Believing is seeing: expectations alter visual awareness. *Curr. Biol.* **18**, R697–8 (2008).
14. Kok, P., Brouwer, G. J., van Gerven, M. A. J. & de Lange, F. P. Prior expectations bias sensory

representations in visual cortex. *J. Neurosci.* **33**, 16275–16284 (2013).

15. Khalsa, S. S. *et al.* Interoception and Mental Health: A Roadmap. *Biol Psychiatry Cogn Neurosci Neuroimaging* **3**, 501–513 (2018).
16. Stephan, K. E. *et al.* Allostatic Self-efficacy: A Metacognitive Theory of Dyshomeostasis-Induced Fatigue and Depression. *Front. Hum. Neurosci.* **10**, 550 (2016).
17. Unal, O. *et al.* Inference on homeostatic belief precision. *Biol. Psychol.* **165**, 108190 (2021).
18. Tenenbaum, J. B., Kemp, C., Griffiths, T. L. & Goodman, N. D. How to grow a mind: statistics, structure, and abstraction. *Science* **331**, 1279–1285 (2011).
19. Griffiths, T. L., Kemp, C. & Tenenbaum, J. B. Bayesian models of cognition. in *The Cambridge handbook of computational psychology (pp* (ed. Sun, R.) vol. 753 59–100 (Cambridge University Press, xii, New York, NY, US, 2008).
20. Sprevak, M. & Smith, R. An Introduction to Predictive Processing Models of Perception and Decision-Making. *Top. Cogn. Sci.* (2023) doi:10.1111/tops.12704.
21. Friston, K., FitzGerald, T., Rigoli, F., Schwartenbeck, P. & Pezzulo, G. Active Inference: A Process Theory. *Neural Comput.* **29**, 1–49 (2017).
22. Pouget, A., Beck, J. M., Ma, W. J. & Latham, P. E. Probabilistic brains: knowns and unknowns. *Nat. Neurosci.* **16**, 1170–1178 (2013).
23. Petzschner, F. H., Glasauer, S. & Stephan, K. E. A Bayesian perspective on magnitude estimation. *Trends Cogn. Sci.* **19**, 285–293 (2015).
24. Onysk, J. *et al.* Statistical learning shapes pain perception and prediction independently of external cues. *Elife* **12**, (2024).
25. Grahl, A., Onat, S. & Büchel, C. The periaqueductal gray and Bayesian integration in placebo analgesia. *Elife* **7**, (2018).
26. Pollo, A. *et al.* Response expectancies in placebo analgesia and their clinical relevance. *Pain* **93**, 77–84 (2001).
27. Peng, W., Peng, H., Lu, J., Fan, B. & Cui, F. Others' Pain Appraisals Modulate the Anticipation and

Experience of Subsequent Pain. *Neuroscience* **410**, 16–28 (2019).

28. Hoskin, R. *et al.* Sensitivity to pain expectations: A Bayesian model of individual differences. *Cognition* **182**, 127–139 (2019).
29. Oka, S. *et al.* Predictability of painful stimulation modulates subjective and physiological responses. *J. Pain* **11**, 239–246 (2010).
30. Zaman, J., Vanpaemel, W., Aelbrecht, C., Tuerlinckx, F. & Vlaeyen, J. W. S. Biased pain reports through vicarious information: A computational approach to investigate the role of uncertainty. *Cognition* **169**, 54–60 (2017).
31. Quelhas Martins, A., McIntyre, D. & Ring, C. Aversive event unpredictability causes stress-induced hypoalgesia. *Psychophysiology* **52**, 1066–1070 (2015).
32. Poublan-couzardot, A., Pagnoni, G. & Lutz, A. Modulation of the sensory and affective dimensions of pain by expectations and uncertainty: a Bayesian modeling approach. (2022) doi:10.31219/osf.io/nteg7.
33. Pavy, F., Zaman, J., Von Leupoldt, A. & Torta, D. M. Expectations underlie the effects of unpredictable pain: a behavioral and electroencephalogram study. *Pain* **165**, 596–607 (2024).
34. Pavy, F. *et al.* The effect of unpredictability on the perception of pain: a systematic review and meta-analysis. *Pain* 10.1097/j.pain.0000000000003199 (2022).
35. Zaman, J., Van Oudenhove, L. & Vlaeyen, J. W. S. Uncertainty in a context of pain: disliked but also more painful? *Pain* **162**, 995–998 (2021).
36. Schenk, L. A. & Colloca, L. The neural processes of acquiring placebo effects through observation. *Neuroimage* **209**, 116510 (2020).
37. Raghuraman, N. *et al.* Neuropsychological mechanisms of observational learning in human placebo effects. *Psychopharmacology* (2024) doi:10.1007/s00213-024-06608-7.
38. Colloca, L. & Benedetti, F. Placebo analgesia induced by social observational learning. *Pain* **144**, 28–34 (2009).
39. Olsson, A. & Phelps, E. A. Social learning of fear. *Nat. Neurosci.* **10**, 1095–1102 (2007).

40. Bajcar, E. A. & Bąbel, P. Social Learning of Placebo Effects in Pain: A Critical Review of the Literature and a Proposed Revised Model. *J. Pain* 104585 (2024).

41. Klauß, H., Kunkel, A., Müßgens, D., Haaker, J. & Bingel, U. Learning by observing: a systematic exploration of modulatory factors and the impact of observationally induced placebo and nocebo effects on treatment outcomes. *Front. Psychol.* **15**, 1293975 (2024).

42. de Gardelle, V. & Summerfield, C. Robust averaging during perceptual judgment. *Proc. Natl. Acad. Sci. U. S. A.* **108**, 13341–13346 (2011).

43. Spitzer, B., Waschke, L. & Summerfield, C. Selective overweighting of larger magnitudes during noisy numerical comparison. *Nat Hum Behav* **1**, 145 (2017).

44. Eippert, F. *et al.* Activation of the Opioidergic Descending Pain Control System Underlies Placebo Analgesia. *Neuron* **63**, 533–543 (2009).

45. Geuter, S. & Büchel, C. Facilitation of pain in the human spinal cord by nocebo treatment. *J. Neurosci.* **33**, 13784–13790 (2013).

46. Tinnermann, A., Geuter, S., Sprenger, C., Finsterbusch, J. & Büchel, C. Interactions between brain and spinal cord mediate value effects in nocebo hyperalgesia. *Science* **358**, 105–108 (2017).

47. Zunhammer, M., Spisák, T., Wager, T. D., Bingel, U. & Placebo Imaging Consortium. Meta-analysis of neural systems underlying placebo analgesia from individual participant fMRI data. *Nat. Commun.* **12**, 1391 (2021).

48. Kok, P., Mostert, P. & de Lange, F. P. Prior expectations induce prestimulus sensory templates. *Proc. Natl. Acad. Sci. U. S. A.* **114**, 10473–10478 (2017).

49. Zunhammer, M., Bingel, U., Wager, T. D. & Placebo Imaging Consortium. Placebo Effects on the Neurologic Pain Signature: A Meta-analysis of Individual Participant Functional Magnetic Resonance Imaging Data. *JAMA Neurol.* **75**, 1321–1330 (2018).

50. Wager, T. D., Atlas, L. Y., Leotti, L. A. & Rilling, J. K. Predicting individual differences in placebo analgesia: contributions of brain activity during anticipation and pain experience. *J. Neurosci.* **31**, 439–452 (2011).

51. Firestone, C. & Scholl, B. J. Cognition does not affect perception: Evaluating the evidence for 'top-down' effects. *Behav. Brain Sci.* **39**, e229 (2016).

52. Wager, T. D. & Lauren Y. Atlas. The neuroscience of placebo effects: connecting context, learning and health. *Nat. Rev. Neurosci.* **16**, 403–418 (2015).

53. Geuter, S., Koban, L. & Wager, T. D. The Cognitive Neuroscience of Placebo Effects: Concepts, Predictions, and Physiology. *Annu. Rev. Neurosci.* **40**, 167–188 (2017).

54. Price, D. D., Finniss, D. G. & Benedetti, F. A comprehensive review of the placebo effect: recent advances and current thought. *Annu. Rev. Psychol.* **59**, 565–590 (2008).

55. Botvinik-Nezer, R. *et al.* Placebo treatment affects brain systems related to affective and cognitive processes, but not nociceptive pain. *bioRxiv* (2023) doi:10.1101/2023.09.21.558825.

56. Roelofs, J., Peters, M. L., Deutz, J., Spijker, C. & Vlaeyen, J. W. S. The Fear of Pain Questionnaire (FPQ): further psychometric examination in a non-clinical sample. *Pain* **116**, 339–346 (2005).

57. Sullivan, M. J. L., Bishop, S. R. & Pivik, J. The Pain Catastrophizing Scale: Development and validation. *Psychol. Assess.* **7**, 524–532 (1995).

58. Spielberger, C. D. Chapter 1 - CURRENT TRENDS IN THEORY AND RESEARCH ON ANXIETY. in *Anxiety* (ed. Spielberger, C. D.) 3–19 (Academic Press, 1972).

59. Jepma, M., Jones, M. & Wager, T. D. The dynamics of pain: evidence for simultaneous site-specific habituation and site-nonspecific sensitization in thermal pain. *J. Pain* **15**, 734–746 (2014).

60. Jepma, M. & Wager, T. D. Conceptual Conditioning: Mechanisms Mediating Conditioning Effects on Pain. *Psychol. Sci.* **26**, 1728–1739 (2015).

61. Koban, L. & Wager, T. D. Beyond conformity: Social influences on pain reports and physiology. *Emotion* **16**, 24–32 (2016).

62. Jepma, M., Koban, L., van Doorn, J., Jones, M. & Wager, T. D. Behavioural and neural evidence for self-reinforcing expectancy effects on pain. *Nature Human Behaviour* **2**, 838–855 (2018).

63. Wager, T. D. *et al.* An fMRI-based neurologic signature of physical pain. *N. Engl. J. Med.* **368**, 1388–1397 (2013).

64. Han, X. *et al.* Effect sizes and test-retest reliability of the fMRI-based neurologic pain signature. *Neuroimage* **247**, 118844 (2022).

65. Woo, C.-W. *et al.* Quantifying cerebral contributions to pain beyond nociception. *Nat. Commun.* **8**, 14211 (2017).

66. Woo, C.-W., Chang, L. J., Lindquist, M. A. & Wager, T. D. Building better biomarkers: brain models in translational neuroimaging. *Nat. Neurosci.* **20**, 365–377 (2017).

67. Kober, H., Buhle, J., Weber, J., Ochsner, K. N. & Wager, T. D. Let it be: mindful acceptance down-regulates pain and negative emotion. *Soc. Cogn. Affect. Neurosci.* **14**, 1147–1158 (2019).

68. Roy, M. *et al.* Representation of aversive prediction errors in the human periaqueductal gray. *Nat. Neurosci.* **17**, 1607–1612 (2014).

69. Jepma, M., Roy, M., Ramlakhan, K., van Velzen, M. & Dahan, A. Different brain systems support learning from received and avoided pain during human pain-avoidance learning. *Elife* **11**, (2022).

70. Mulders, D., Seymour, B., Mouraux, A. & Mancini, F. Confidence of probabilistic predictions modulates the cortical response to pain. *Proc. Natl. Acad. Sci. U. S. A.* **120**, e2212252120 (2023).

71. Mancini, F., Zhang, S. & Seymour, B. Computational and neural mechanisms of statistical pain learning. *Nat. Commun.* **13**, 6613 (2022).

72. Brown, C. A., Seymour, B., Boyle, Y., El-Deredy, W. & Jones, A. K. P. Modulation of pain ratings by expectation and uncertainty: Behavioral characteristics and anticipatory neural correlates. *Pain* **135**, 240–250 (2008).

73. Winkler, I. & Schröger, E. Auditory perceptual objects as generative models: Setting the stage for communication by sound. *Brain Lang.* **148**, 1–22 (2015).

74. Winkler, I., Denham, S. L. & Nelken, I. Modeling the auditory scene: predictive regularity representations and perceptual objects. *Trends Cogn. Sci.* **13**, 532–540 (2009).

75. Nobre, A., Correa, A. & Coull, J. The hazards of time. *Curr. Opin. Neurobiol.* **17**, 465–470 (2007).

76. Nitschke, J. B. *et al.* Altering expectancy dampens neural response to aversive taste in primary taste cortex. *Nat. Neurosci.* **9**, 435–442 (2006).

77. van de Sand, M. F., Menz, M. M., Sprenger, C. & Büchel, C. Nocebo-induced modulation of cerebral itch processing - An fMRI study. *Neuroimage* **166**, 209–218 (2018).

78. Colagiuri, B. & Zachariae, R. Patient expectancy and post-chemotherapy nausea: a meta-analysis. *Ann. Behav. Med.* **40**, 3–14 (2010).

79. Rao, R. P. & Ballard, D. H. Predictive coding in the visual cortex: a functional interpretation of some extra-classical receptive-field effects. *Nat. Neurosci.* **2**, 79–87 (1999).

80. Iordanova, M. D., Yau, J. O.-Y., McDannald, M. A. & Corbit, L. H. Neural substrates of appetitive and aversive prediction error. *Neurosci. Biobehav. Rev.* **123**, 337–351 (2021).

81. Seymour, B. *et al.* Temporal difference models describe higher-order learning in humans. *Nature* **429**, 664–667 (2004).

82. Orne, M. On the Social Psychology of the Psychological Experiment. *Am. Psychol.* **17**, 776–783 (1962).

83. Öztel, T. & Balcı, F. Bayes Optimal Integration of Social and Endogenous Uncertainty in Numerosity Estimation. *Cogn. Sci.* **48**, e13447 (2024).

84. Göbel, K., Hensel, L., Schultheiss, O. C. & Niessen, C. Meta-analytic evidence shows no relationship between task-based and self-report measures of thought control. *Appl. Cogn. Psychol.* **36**, 659–672 (2022).

85. Enkavi, A. Z. *et al.* Large-scale analysis of test-retest reliabilities of self-regulation measures. *Proc. Natl. Acad. Sci. U. S. A.* **116**, 5472–5477 (2019).

86. Friedman, N. P. & Banich, M. T. Questionnaires and task-based measures assess different aspects of self-regulation: Both are needed. *Proceedings of the National Academy of Sciences of the United States of America* vol. 116 24396–24397 (2019).

87. Wennerhold, L. & Friese, M. Why Self-Report Measures of Self-Control and Inhibition Tasks Do Not Substantially Correlate. *Collabra: Psychology* **6**, 9 (2020).

88. Brainard, D. H. The Psychophysics Toolbox. *Spat. Vis.* **10**, 433–436 (1997).

89. Bates, D., Mächler, M., Bolker, B. & Walker, S. Fitting Linear Mixed-Effects Models Using lme4. *J.*

Stat. Softw. **67**, 1–48 (2015).

90. Kuznetsova, A., Brockhoff, P. B. & Christensen, R. H. B. LmerTest package: Tests in linear mixed effects models. *J. Stat. Softw.* **82**, (2017).
91. Barr, D. J., Levy, R., Scheepers, C. & Tily, H. J. Random effects structure for confirmatory hypothesis testing: Keep it maximal. *J. Mem. Lang.* **68**, (2013).
92. Matuschek, H., Kliegl, R., Vasishth, S., Baayen, H. & Bates, D. Balancing Type I error and power in linear mixed models. *J. Mem. Lang.* **94**, 305–315 (2017).
93. Esteban, O. *et al.* fMRIPrep: a robust preprocessing pipeline for functional MRI. *Nat. Methods* **16**, 111–116 (2019).
94. Esteban, O. *et al.* poldracklab/fmriprep: 1.0.8. (2018) doi:10.5281/ZENODO.1183390.
95. Gorgolewski, K. *et al.* Nipype: a flexible, lightweight and extensible neuroimaging data processing framework in python. *Front. Neuroinform.* **5**, 13 (2011).
96. Esteban, O. *et al. Nipy/nipype: 1.8.3*. (2022). doi:10.5281/zenodo.6834519.
97. Tustison, N. J. *et al.* N4ITK: improved N3 bias correction. *IEEE Trans. Med. Imaging* **29**, 1310–1320 (2010).
98. Avants, B. B., Epstein, C. L., Grossman, M. & Gee, J. C. Symmetric diffeomorphic image registration with cross-correlation: evaluating automated labeling of elderly and neurodegenerative brain. *Med. Image Anal.* **12**, 26–41 (2008).
99. Zhang, Y., Brady, M. & Smith, S. Segmentation of brain MR images through a hidden Markov random field model and the expectation-maximization algorithm. *IEEE Trans. Med. Imaging* **20**, 45–57 (2001).
100. Fonov, V. S., Evans, A. C., McKinstry, R. C., Almli, C. R. & Collins, D. L. Unbiased nonlinear average age-appropriate brain templates from birth to adulthood. *Neuroimage* **47**, S102 (2009).
101. Jenkinson, M. & Smith, S. A global optimisation method for robust affine registration of brain images. *Med. Image Anal.* **5**, 143–156 (2001).
102. Greve, D. N. & Fischl, B. Accurate and robust brain image alignment using boundary-based

registration. *Neuroimage* **48**, 63–72 (2009).

103. Jenkinson, M., Bannister, P., Brady, M. & Smith, S. Improved Optimization for the Robust and Accurate Linear Registration and Motion Correction of Brain Images. *Neuroimage* **17**, 825–841 (2002).

104. Power, J. D. *et al.* Methods to detect, characterize, and remove motion artifact in resting state fMRI. *Neuroimage* **84**, 320–341 (2014).

105. Abraham, A. *et al.* Machine Learning for Neuroimaging with Scikit-Learn. *Frontiers in Neuroinformatics* **8**, 1–10 (2014).

106. Rissman, J., Gazzaley, A. & D'Esposito, M. Measuring functional connectivity during distinct stages of a cognitive task. *Neuroimage* **23**, 752–763 (2004).

107. Shrout, P. E. & Bolger, N. Mediation in experimental and nonexperimental studies: new procedures and recommendations. *Psychol. Methods* **7**, 422–445 (2002).

Supplementary Information

Expectation generation and its effect on subsequent pain and visual perception

Rotem Botvinik-Nezer[1,2,*], Stephan Geuter[3], Martin A. Lindquist[3] and Tor D. Wager[2,*]

[1]Hebrew University of Jerusalem; [2]Dartmouth College; [2]Johns Hopkins University;

[*]Corresponding authors

Supplementary Results

Computational Modeling of Perception

We developed five computational models to test whether and how cue-based expectations are weighted when performing perception, whether the effect of expectations persist, and whether these processes are the same or different across modalities. In all models, expectations were computed for each trial of each participant based on the cue, with the optimized participant-level model from the expectation data. The intensity-based (expectation-independent) rating of each stimulus was determined based on the mean rating of each participant for a given intensity in the stimulus-response task, with a free parameter s per modality (s_p for pain and s_v for vision) that serves as a linear scaling factor, to account for the different context between the stimulus-response and cued-perception tasks (e.g., outside vs. inside the MRI scanner) and physiological processes (e.g., habituation or differences in sensitivity across skin sites).

The Baseline Model assumes the cue-based expectations do not affect perception throughout the task, and thus the rating is only based on the stimulus intensity and the scaling factor. In the Expectation Model, there are significant cue effects, and perception is based on a combination of the stimulus intensity and the cue-based expectations, with a free parameter w which is fixed throughout the task for each participant. This parameter determines the weight given to cue-based expectations vs. incoming information (stimulus intensity). In the "Expectation Learning Model", there are also significant cue effects, and the relative contribution of expectation vs. stimulus intensity at the beginning of the task is determined by the free parameter $w0$. Then, w is updated from trial to trial based on prediction errors between the expected and empirical rating, with learning rate α. The two last models are equivalent to the second and third models, but include separate free parameters for each modality. In the "Expectation Model by Modality", w_p and w_v model the weighting of expectations for pain and visual perception trials, respectively. In the "Expectation Learning Model by Modality", $w0_p$ and $w0_v$ model the initial weighting of the expectation in each modality, and α_p and α_v model the learning rate for the pain and visual perception, respectively.

We fit each model to each participant's data from the cued-perception task, and optimized the free parameters based on ordinal least squares between the predicted and empirical ratings of the

painfulness or visual contrast of the stimulus. We also compared the five models and selected the best model for each participant based on F tests for nested models. Of 45 participants, the Baseline Model was the best model for 8 participants (18% of sample), the Expectation Model was best for 16 participants (35%), the Expectation Learning Model was best for 5 participants (11%), the Expectation Model by Modality was best for 8 participants (18%), and the Expectation Learning Model by Modality was best for 8 participants (18%).

In line with the participant-level results, group-level F tests for nested models based on the residual sum of squares indicated that the Expectation Model fits the data significantly better than the Baseline model ($F = 12.40$, $p = .001$), but the more complex models do not significantly improve the fit (Expectation Model vs. Expectation Learning Model: $F = 2.04$, $p = .161$; Expectation Model vs. Expectation Model by Modality: $F = 1.06$, $p = .309$; Expectation Model by Modality vs. Expectation Learning Model by Modality: $F = 1.47$, $p = .242$). Comparison based on the Akaike Information Criterion (AIC) indicated that the Expectation Model and the Expectation Learning Model were the best models while accounting for complexity (AIC values: Baseline Model = 309.81; Expectation Model = 300.17; Expectation Learning Model = 299.99 Expectation Model by Modality = 301.02; Expectation Learning Model by Modality = 301.75). These results suggest that the cues affected participants' perception, and that only some participants learned to downweight (or ignore) the cues during the task. They further suggest that these processes were largely similar across modalities.

Finally, a direct comparison of w_p and w_v showed that participants weighted the cues more in pain than visual trials (paired t-test, mean difference = 0.090, *SD* difference = 0.191, *Cohen's d* = 0.471, $t_{(44)} = 3.162$, $p = .003$), indicating greater influences of cues on pain perception than visual perception, though cue effects were strong in both modalities.

Effects on neural perceptual processing

In addition to the results reported in the main text, we further tested "off target" effects–stimulus intensity and cue effects on visual regions during pain perception, or pain regions during visual perception. Activity was higher (less negative) during more intense heat stimuli in several visual regions, probably because noxious stimuli produce diffuse effects, but none of them was affected

by the cue during pain perception. Activity in the right IPS was higher during pain perception following cues with lower mean (similar to the aversive PE-like activity in the PAG; $p = .047$). Conversely, activity during visual perception was not affected by the stimulus intensity in any of the pain processing regions (all ps $\geq .162$), but it was higher following cues with lower mean in the right VPL/VPM thalamus ($p = .046$), and lower following negatively skewed compared to symmetric cues in the right dorsal posterior insula ($p = .001$) and right S1 ($p = .018$). In addition, there was a significant cue mean x cue variance interaction effect on activity in the right NAc (shell-like) during visual perception ($p = .048$), such that activity was slightly more negative following high compared to low mean for low variance cues, but less negative for high compared to low mean for high variance cues (not in line with Bayesian predictive coding accounts).

Effects on anticipatory neural activity

While both the current study and most previous ones focused on cue effects on stimulus-evoked activity, we also performed an exploratory analysis to test anticipatory activity (see Supplementary Figure 3 and Supplementary Figure 4). Several pain processing regions were more active during anticipation in response to high vs. low cue mean, including the dorsal posterior insula (right $p = .030$; left $p = .039$), aMCC ($p = .008$), PAG ($p = .049$), and anterior insula (right $p = .023$; left $p = .010$). In addition, cue-evoked activity in the PAG ($p = .043$) and NAc (core-like; right $p = .020$; left $p = .049$) was lower following positively skewed compared to symmetric cues (opposite direction than expected and observed behaviorally, although it was not significant behaviorally). On visual trials, anticipatory activity was lower following high vs. low cue mean in V4 (right $p = .025$; left $p = .028$), left V5 ($p = .001$), left VMV2 ($p = .003$), left VMV3 ($p = .017$), left V3B ($p = .005$), left V4t ($p = .001$), IPS (right $p = .001$; left $p = .034$), and left dlPFC ($p = .046$). It was also higher for cues with higher variance (less certain cues) in right V4 ($p = .020$), left NAc (core-like, $p = .017$) and VPL/VPM thalamus (right $p = .046$, left $p = .038$). As for the skewness, anticipatory activity in visual trials was higher for negatively skewed compared to symmetric cues (opposite from the behavioral direction) in the right IPS ($p = .006$) and lower for positively skewed compared to symmetric cues (again, opposite from the behavioral effect) in the right NAc (core-like $p = .004$; shell-like $p = .018$). Finally, there was a significant interaction between the cue mean and the cue variance in the right VMV3 ($p = .042$), such that anticipatory activity was higher for high compared

to low cue mean for more certain cues, and higher for low compared to high cue mean for less certain cues (not in line with Bayesian predictive coding accounts).

Supplementary Figure 1. Stimulus intensity and cue effects across all ROIs during thermal stimuli. Asterisks represent the level of significance (* $p < .05$, ** $p < .01$, *** $p < .001$). Abbreviations: Neg = negative; Pos = positive; Sym = symmetric; NPS = Neurological Brain Signature; SIIPS = Stimulus Intensity Independent Pain Signature; VPL/VPM = ventral posterior lateral/medial; Thal = thalamus; dpIns = dorsal posterior insula; aIns = anterior insula; aMCC = anterior midcingulate cortex; PAG = periaqueductal gray; IPS = intraparietal sulcus; OFC = orbitofrontal cortex; dlPFC = dorsolateral prefrontal cortex; NAc = nucleus accumbens.

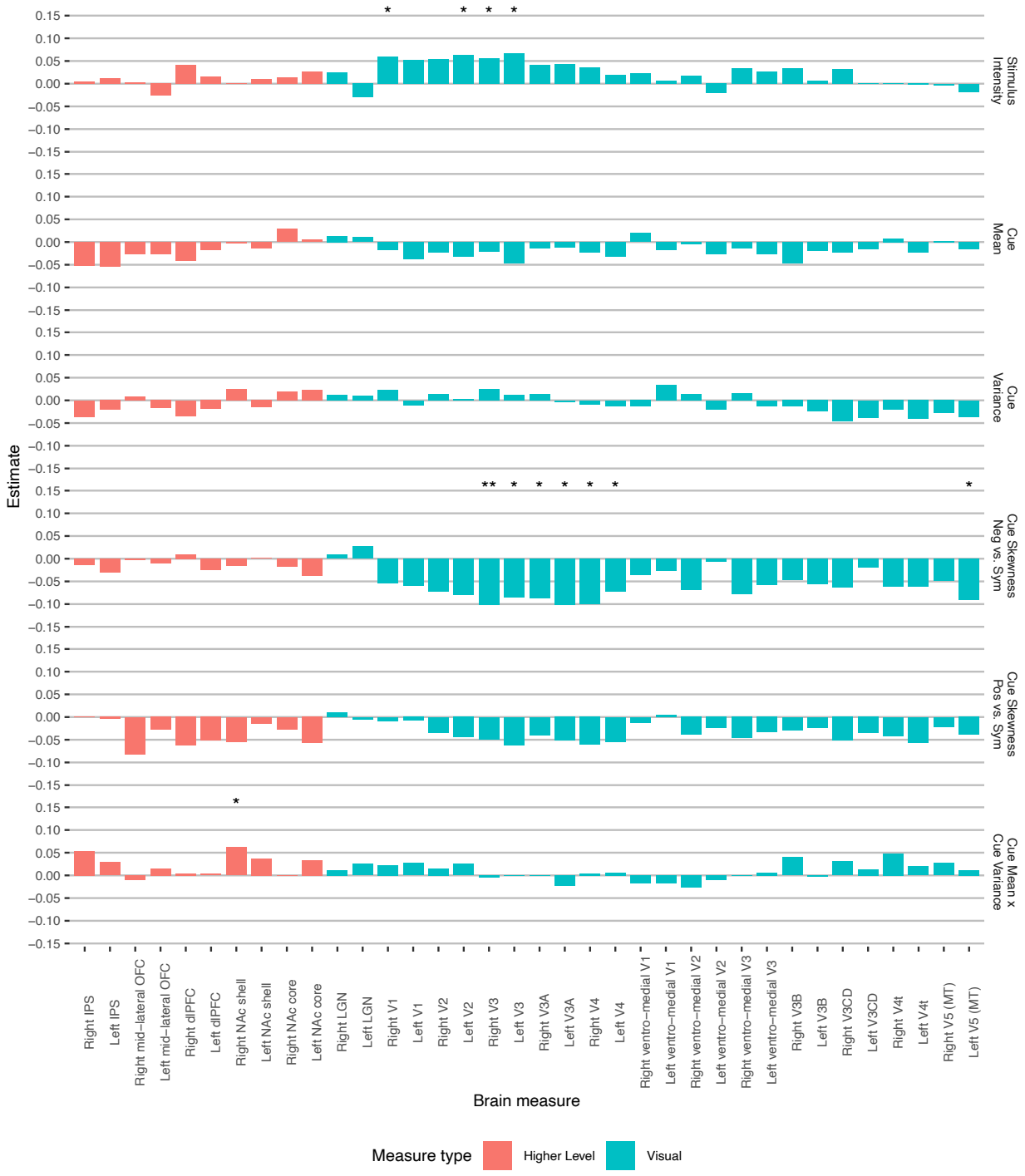

Supplementary Figure 2. Stimulus intensity and cue effects across all ROIs during visual stimuli. Asterisks represent the level of significance (* $p < .05$, ** $p < .01$, *** $p < .001$). Abbreviations: Neg = negative; Pos = positive; Sym = symmetric; IPS = intraparietal sulcus; OFC = orbitofrontal cortex; dlPFC = dorsolateral prefrontal cortex; NAc = nucleus accumbens; LGN = lateral geniculate nucleus.

Supplementary Figure 3. Cue effects across all ROIs during anticipation for thermal stimuli. Asterisks represent the level of significance (* $p < .05$, ** $p < .01$, *** $p < .001$). Abbreviations: Neg = negative; Pos = positive; Sym = symmetric; NPS = Neurological Brain Signature; SIIPS = Stimulus Intensity Independent Pain Signature; VPL/VPM = ventral posterior lateral/medial; Thal = thalamus; dpIns = dorsal posterior insula; aIns = anterior insula; aMCC = anterior midcingulate cortex; PAG = periaqueductal gray; IPS = intraparietal sulcus; OFC = orbitofrontal cortex; dlPFC = dorsolateral prefrontal cortex; NAc = nucleus accumbens.

Supplementary Figure 4. Cue effects across all ROIs during anticipation for visual stimuli. Asterisks represent the level of significance (* $p < .05$, ** $p < .01$, *** $p < .001$). Abbreviations: Neg = negative; Pos = positive; Sym = symmetric; IPS = intraparietal sulcus; OFC = orbitofrontal cortex; dlPFC = dorsolateral prefrontal cortex; NAc = nucleus accumbens; LGN = lateral geniculate nucleus.

Supplementary Table 1. A priori regions of interest. Atlases are available via CANlab neuroimaging analysis tools (https://canlab.github.io/). The canlab2023 atlas is used with threshold = 0.2, and its regions included here are based on Glasser2016HCP atlas [1] for cortical regions, Tian2020 atlas [2] for the NAc, and Morel2010 atlas [3] for the thalamus.

Type	Region	Label
Early nociceptive pain processing (pain pathways atlas)	Dorsal posterior insula (dpIns)	dpIns_L, dpIns_R
	Ventral posterior thalamus	Thal_VPLM_L, Thal_VPLM_R
Nociceptive pain processing (pain pathways atlas)	Periaqueductal gray (PAG)	Bstem_PAG
	Anterior midcingulate cortex (aMCC)	aMCC_MPFC
	Medial thalamus	Thal_MD
Higher-level pain processing (canlab2023 atlas based on Glasser2016HCP atlas [1] for cortical regions and	Nucleus accumbens (NAc) - shell	NAc_shell_like_L, NAc_shell_like_R
	Nucleus accumbens (NAc) - core	NAc_core_like_L, NAc_core_like_R
	Mid lateral orbitofrontal cortex (OFC)	Ctx_11l_L, Ctx_11l_R
	dlPFC	Left: Ctx_8C_L and Ctx_46_L; Right: Ctx_p9_46v_R
Other pain processing (pain pathways atlas)	Primary somatosensory (S1), mostly hand area	s1_handplus_L, s1_handplus_R
	Anterior insula (aIns)	aIns_L, aIns_R
Early visual processing (canlab2023_coarse_2mm atlas)	Lateral geniculate nucleus (LGN)	Thal_Lateral_Geniculate_Nucleus_L, Thal_Lateral_Geniculate_Nucleus_R
	Primary visual cortex (V1)	Ctx_V1_L,Ctx_V1_R
	Secondary visual cortex (V2)	Ctx_V2_L,Ctx_V2_R
Visual processing (canlab2023_coarse_2mm atlas)	V3	Ctx_V3_L, Ctx_V3_R
	V4	Ctx_V4_L, Ctx_V4_R
	Middle temporal visual area V5 (MT)	Ctx_MT_L, Ctx_MT_R
Higher-level visual processing (canlab2023_coarse_2mm atlas)	Intraparietal sulcus (IPS)	Ctx_IPS1_L, Ctx_IPS1_R
Other visual processing (canlab2023_coarse_2mm atlas)	VMV1	Ctx_VMV1_L, Ctx_VMV1_R
	VMV2	Ctx_VMV2_L, Ctx_VMV2_R
	V3A	Ctx_V3A_L, Ctx_V3A_R
	V3B	Ctx_V3B_L, Ctx_V3B_R
	V3CD	Ctx_V3CD_L, Ctx_V3CD_R
	VMV3	Ctx_VMV3_L, Ctx_VMV3_R
	V4t	Ctx_V4t_L, Ctx_V4t_R

Supplementary Table 2. Statistics for the effects on NPS and SIIPS scores during visual perception.

Neuromarker	Effect	Estimate	SE	DF	t	p
NPS	Stimulus Intensity	-0.015	0.030	2947.1	-0.50	0.617
	Cue mean	-0.013	0.030	2946.4	-0.45	0.652
	Cue var	0.022	0.030	2947.9	0.75	0.456
	Cue SK (neg)	-0.055	0.042	2947.4	-1.29	0.196
	Cue SK (pos)	0.038	0.042	2947.3	0.90	0.368
	Cue mean x cue var	0.000	0.030	2946.4	0.02	0.988
SIIPS	Stimulus Intensity	-0.027	0.030	2935.7	-0.88	0.377
	Cue mean	-0.005	0.030	2935.1	-0.17	0.864
	Cue var	0.051	0.030	2936.7	1.68	0.094
	Cue SK (neg)	0.008	0.043	2936.1	0.20	0.844
	Cue SK (pos)	0.035	0.043	2935.9	0.81	0.417
	Cue mean x cue var	-0.011	0.030	2934.9	-0.38	0.704

Supplementary Table 3. Statistics for the effects on ROIs related to early pain perceptual processing. Abbreviations: var = variance; SK = skewness; neg = negative (vs. symmetric); pos = positive (vs. symmetric); stim int = stimulus intensity; VPL/VPM Thal = ventral posterior thalamus (medial and lateral); dpIns = dorsal posterior insula. Significant effects (uncorrected $p < .05$) are marked in bold.

Region	Effect	Estimate	SE	DF	t	p
Left dpIns	**Stimulus intensity**	**0.145**	**0.028**	**2906.0**	**5.17**	**< .001**
	Cue mean	-0.016	0.029	302.1	-0.55	0.585
	Cue var	0.002	0.028	2905.7	0.06	0.956
	Cue SK (neg)	0.030	0.040	2905.3	0.76	0.444
	Cue SK (pos)	0.005	0.040	2906.3	0.14	0.892
	Cue mean x cue var	-0.005	0.028	2913.9	-0.18	0.858
	Stim int x cue mean	-0.001	0.028	2904.7	-0.05	0.963
Left VPL/VPM Thal	**Stimulus intensity**	**0.084**	**0.029**	**2906.8**	**2.93**	**0.003**
	Cue mean	-0.043	0.029	314.4	-1.47	0.141
	Cue var	0.001	0.029	2906.6	0.05	0.962
	Cue SK (neg)	0.013	0.040	2906.1	0.31	0.757
	Cue SK (pos)	-0.005	0.040	2907.2	-0.13	0.898
	Cue mean x cue var	0.006	0.029	2914.8	0.22	0.830
	Stim int x cue mean	0.005	0.029	2905.6	0.17	0.862
Right dpIns	**Stimulus intensity**	**0.155**	**0.027**	**2948.3**	**5.67**	**< .001**
	Cue mean	-0.027	0.027	2948.6	-1.00	0.316
	Cue var	-0.019	0.027	2949.1	-0.68	0.499
	Cue SK (neg)	0.012	0.039	2948.6	0.31	0.754
	Cue SK (pos)	0.030	0.039	2948.8	0.78	0.435
	Cue mean x cue var	-0.003	0.027	2948.5	-0.10	0.916
	Stim int x cue mean	-0.007	0.027	2948.7	-0.24	0.808
Right VPL/VPM Thal	**Stimulus intensity**	**0.112**	**0.029**	**2946.5**	**3.88**	**< .001**
	Cue mean	-0.025	0.029	2946.9	-0.87	0.385
	Cue var	0.008	0.029	2947.7	0.28	0.783
	Cue SK (neg)	-0.031	0.041	2946.9	-0.75	0.456
	Cue SK (pos)	-0.045	0.041	2947.3	-1.10	0.273
	Cue mean x cue var	-0.006	0.029	2946.8	-0.21	0.836
	Stim int x cue mean	-0.027	0.029	2947.0	-0.94	0.346

Supplementary Table 4. Statistics for the effects on ROIs related to early visual perceptual processing. Abbreviations: var = variance; SK = skewness; neg = negative (vs. symmetric); pos = positive (vs. symmetric); stim int = stimulus intensity; LGN = lateral geniculate nucleus. Significant effects (uncorrected $p < .05$) are marked in bold.

Region	Effect	Estimate	SE	DF	t	p
Right LGN	Stimulus Intensity	0.024	0.031	2926.4	0.78	0.438
	Cue mean	0.013	0.031	308.5	0.41	0.683
	Cue var	0.012	0.031	2926.1	0.40	0.687
	Cue SK (neg)	0.009	0.043	2926.0	0.21	0.837
	Cue SK (pos)	0.010	0.043	2925.8	0.23	0.819
	Cue mean x var	0.012	0.031	2927.4	0.38	0.702
	Stim int x cue mean	-0.014	0.031	2927.1	-0.46	0.646
Left LGN	Stimulus Intensity	-0.030	0.031	2963.7	-0.97	0.332
	Cue mean	0.010	0.031	2962.8	0.34	0.736
	Cue var	0.011	0.031	2963.8	0.37	0.712
	Cue SK (neg)	0.027	0.044	2963.3	0.63	0.531
	Cue SK (pos)	-0.005	0.043	2963.7	-0.12	0.902
	Cue mean x var	0.025	0.031	2962.7	0.81	0.418
	Stim int x cue mean	-0.023	0.031	2962.8	-0.75	0.456
Right V1	**Stimulus Intensity**	**0.059**	**0.029**	**2947.0**	**2.04**	**0.041**
	Cue mean	-0.017	0.029	2946.4	-0.58	0.563
	Cue var	0.022	0.029	2947.0	0.78	0.438
	Cue SK (neg)	-0.054	0.041	2946.8	-1.32	0.187
	Cue SK (pos)	-0.009	0.041	2946.6	-0.23	0.821
	Cue mean x var	0.022	0.029	2946.3	0.75	0.456
	Stim int x cue mean	-0.032	0.029	2946.4	-1.11	0.269
Left V1	Stimulus Intensity	0.053	0.029	2951.0	1.83	0.067
	Cue mean	-0.037	0.029	2950.4	-1.27	0.204
	Cue var	-0.011	0.029	2951.0	-0.39	0.696
	Cue SK (neg)	-0.059	0.041	2950.8	-1.43	0.153
	Cue SK (pos)	-0.008	0.041	2950.6	-0.21	0.838
	Cue mean x var	0.027	0.029	2950.4	0.94	0.348
	Stim int x cue mean	-0.031	0.029	2950.4	-1.06	0.289
Right V2	Stimulus Intensity	0.054	0.028	2956.6	1.89	0.058
	Cue mean	-0.023	0.028	2956.1	-0.80	0.423
	Cue var	0.013	0.028	2956.5	0.46	0.646
	Cue SK (neg)	-0.072	0.040	2956.4	-1.80	0.072
	Cue SK (pos)	-0.034	0.040	2956.3	-0.84	0.401
	Cue mean x var	0.015	0.028	2956.0	0.51	0.608
	Stim int x cue mean	-0.021	0.028	2956.1	-0.74	0.461
Left V2	**Stimulus Intensity**	**0.064**	**0.029**	**2953.0**	**2.20**	**0.028**
	Cue mean	-0.032	0.029	2952.4	-1.09	0.275
	Cue var	0.003	0.029	2953.0	0.11	0.916
	Cue SK (neg)	-0.079	0.041	2952.8	-1.92	0.056
	Cue SK (pos)	-0.044	0.041	2952.6	-1.08	0.282
	Cue mean x var	0.025	0.029	2952.4	0.85	0.395
	Stim int x cue mean	-0.021	0.029	2952.4	-0.74	0.460

Supplementary Table 5. Statistics for the effects on ROIs related to pain perceptual processing. Abbreviations: var = variance; SK = skewness; neg = negative (vs. symmetric); pos = positive (vs. symmetric); stim int = stimulus intensity; aMCC = anterior midcingulate cortex; Med Thal = medial thalamus; PAG = periaqueductal gray. Significant effects (uncorrected $p < .05$) are marked in bold.

Region	Effect	Estimate	SE	DF	t	p
aMCC	**Stimulus Intensity**	**0.109**	**0.028**	**2905.4**	**3.92**	**< .001**
	Cue mean	-0.010	0.029	243.7	-0.35	0.728
	Cue var	0.001	0.028	2905.0	0.03	0.973
	Cue SK (neg)	0.031	0.039	2904.8	0.79	0.432
	Cue SK (pos)	0.040	0.039	2905.5	1.03	0.303
	Cue mean x var	-0.021	0.028	2912.4	-0.75	0.453
	Stim int x cue mean	-0.029	0.028	2904.1	-1.06	0.291
Med Thal	**Stimulus Intensity**	**0.097**	**0.029**	**2948.5**	**3.34**	**0.001**
	Cue mean	-0.005	0.029	2948.9	-0.16	0.872
	Cue var	-0.027	0.029	2949.8	-0.94	0.347
	Cue SK (neg)	0.017	0.041	2949.0	0.42	0.674
	Cue SK (pos)	-0.017	0.041	2949.4	-0.41	0.680
	Cue mean x var	-0.010	0.029	2948.8	-0.35	0.728
	Stim int x cue mean	-0.010	0.029	2949.1	-0.35	0.726
PAG	**Stimulus Intensity**	**0.141**	**0.030**	**2907.3**	**4.71**	**< .001**
	Cue mean	**-0.066**	**0.030**	**341.9**	**-2.17**	**0.031**
	Cue var	0.054	0.030	2907.8	1.79	0.073
	Cue SK (neg)	0.014	0.042	2906.8	0.33	0.739
	Cue SK (pos)	-0.001	0.042	2907.9	-0.04	0.972
	Cue mean x var	0.025	0.030	2915.3	0.83	0.406
	Stim int x cue mean	-0.028	0.030	2906.4	-0.92	0.357

Supplementary Table 6. Statistics for the effects on ROIs related to visual perceptual processing. Abbreviations: var = variance; SK = skewness; neg = negative (vs. symmetric); pos = positive (vs. symmetric); stim int = stimulus intensity; MT = middle temporal. Significant effects (uncorrected $p < .05$) are marked in bold.

Region	Effect	Estimate	SE	DF	t	p
	Stimulus Intensity	**0.055**	**0.027**	**2961.3**	**2.00**	**0.046**
	Cue mean	-0.021	0.027	2960.9	-0.77	0.439
	Cue var	0.024	0.027	2961.3	0.87	0.386
Right V3	**Cue SK (neg)**	**-0.102**	**0.039**	**2961.2**	**-2.63**	**0.009**
	Cue SK (pos)	-0.049	0.039	2961.1	-1.26	0.207
	Cue mean x var	-0.004	0.027	2960.9	-0.13	0.897
	Stim int x cue mean	-0.018	0.027	2960.9	-0.67	0.505
	Stimulus Intensity	**0.067**	**0.028**	**2955.9**	**2.39**	**0.017**
	Cue mean	-0.046	0.028	2955.5	-1.62	0.106
	Cue var	0.012	0.028	2955.9	0.42	0.672
Left V3	**Cue SK (neg)**	**-0.086**	**0.040**	**2955.7**	**-2.15**	**0.032**
	Cue SK (pos)	-0.062	0.040	2955.6	-1.54	0.123
	Cue mean x var	0.000	0.028	2955.4	-0.01	0.993
	Stim int x cue mean	-0.014	0.028	2955.4	-0.48	0.631
	Stimulus Intensity	0.035	0.027	2953.5	1.30	0.193
	Cue mean	-0.023	0.027	2953.2	-0.84	0.402
	Cue var	-0.009	0.027	2953.6	-0.32	0.747
Right V4	**Cue SK (neg)**	**-0.099**	**0.038**	**2953.5**	**-2.58**	**0.010**
	Cue SK (pos)	-0.061	0.038	2953.4	-1.59	0.111
	Cue mean x var	0.004	0.027	2953.2	0.13	0.894
	Stim int x cue mean	-0.005	0.027	2953.2	-0.18	0.857
	Stimulus Intensity	0.020	0.025	2959.5	0.81	0.421
	Cue mean	-0.032	0.025	2959.2	-1.28	0.201
	Cue var	-0.012	0.025	2959.5	-0.49	0.624
Left V4	**Cue SK (neg)**	**-0.072**	**0.036**	**2959.4**	**-2.01**	**0.045**
	Cue SK (pos)	-0.054	0.036	2959.3	-1.52	0.130
	Cue mean x var	0.006	0.025	2959.2	0.25	0.805
	Stim int x cue mean	0.008	0.025	2959.2	0.33	0.740
	Stimulus Intensity	-0.003	0.029	2957.0	-0.10	0.922
	Cue mean	0.002	0.029	2956.5	0.06	0.954
	Cue var	-0.028	0.029	2957.0	-0.99	0.321
Right V5 (MT)	Cue SK (neg)	-0.048	0.041	2956.9	-1.17	0.242
	Cue SK (pos)	-0.021	0.041	2956.8	-0.51	0.608
	Cue mean x var	0.027	0.029	2956.5	0.94	0.349
	Stim int x cue mean	-0.008	0.029	2956.5	-0.27	0.784
	Stimulus Intensity	-0.018	0.029	2961.1	-0.63	0.531
	Cue mean	-0.015	0.029	2960.7	-0.51	0.607
	Cue var	-0.036	0.029	2961.2	-1.24	0.215
Left V5 (MT)	**Cue SK (neg)**	**-0.091**	**0.041**	**2961.0**	**-2.22**	**0.027**
	Cue SK (pos)	-0.039	0.041	2960.9	-0.95	0.344
	Cue mean x var	0.012	0.029	2960.6	0.43	0.666
	Stim int x cue mean	0.044	0.029	2960.7	1.53	0.126

Supplementary Table 7. Statistics for the effects on ROIs related to higher level pain processing. Abbreviations: var = variance; SK = skewness; neg = negative (vs. symmetric); pos = positive (vs. symmetric); stim int = stimulus intensity; dlPFC = dorsolateral prefrontal cortex; OFC = orbitofrontal cortex; NAc = nucleus accumbens. Significant effects (uncorrected $p < .05$) are marked in bold.

Region	Effect	Estimate	SE	DF	t	p
Right dlPFC	Stimulus Intensity	0.021	0.03	2948.4	0.72	0.473
	Cue mean	-0.026	0.03	2948.8	-0.87	0.386
	Cue var	-0.04	0.03	2949.9	-1.34	0.181
	Cue SK (neg)	0.014	0.042	2949	0.34	0.737
	Cue SK (pos)	-0.007	0.042	2949.4	-0.17	0.868
	Cue mean x var	-0.005	0.03	2948.7	-0.18	0.854
	Stim int x cue mean	0.024	0.03	2949	0.81	0.417
Left dlPFC	**Stimulus Intensity**	**0.098**	**0.03**	**2948.5**	**3.31**	**0.001**
	Cue mean	-0.022	0.03	2948.9	-0.76	0.447
	Cue var	-0.03	0.03	2950	-1.02	0.307
	Cue SK (neg)	0.011	0.042	2949	0.26	0.798
	Cue SK (pos)	0.01	0.042	2949.5	0.25	0.801
	Cue mean x var	0.001	0.03	2948.8	0.05	0.961
	Stim int x cue mean	0.014	0.03	2949.1	0.48	0.631
Right mid-lateral OFC	Stimulus Intensity	-0.009	0.03	2948.5	-0.31	0.757
	Cue mean	0.017	0.03	2948.9	0.58	0.565
	Cue var	-0.049	0.03	2950	-1.64	0.102
	Cue SK (neg)	0.03	0.042	2949	0.72	0.469
	Cue SK (pos)	-0.011	0.042	2949.5	-0.26	0.793
	Cue mean x var	0.003	0.03	2948.8	0.11	0.916
	Stim int x cue mean	0.01	0.03	2949.1	0.32	0.748
Left mid-lateral OFC	Stimulus Intensity	-0.025	0.03	2904.5	-0.85	0.394
	Cue mean	-0.031	0.031	292.8	-1.02	0.308
	Cue var	-0.038	0.03	2904.6	-1.29	0.198
	Cue SK (neg)	0.019	0.042	2903.9	0.46	0.647
	Cue SK (pos)	0.002	0.042	2904.9	0.04	0.97
	Cue mean x var	0.023	0.03	2911.6	0.79	0.432
	Stim int x cue mean	0.028	0.03	2903.4	0.95	0.342
Right NAc core	**Stimulus Intensity**	**0.071**	**0.029**	**2904.9**	**2.39**	**0.017**
	Cue mean	**0.072**	**0.03**	**315.4**	**2.39**	**0.018**
	Cue var	**-0.075**	**0.029**	**2905**	**-2.53**	**0.011**
	Cue SK (neg)	-0.004	0.042	2904.3	-0.11	0.915
	Cue SK (pos)	-0.046	0.042	2905.3	-1.11	0.269
	Cue mean x var	0.047	0.029	2912.8	1.58	0.114
	Stim int x cue mean	-0.02	0.029	2903.8	-0.69	0.49
Right NAc shell	Stimulus Intensity	0.026	0.03	2907.9	0.87	0.384
	Cue mean	0.043	0.031	304.7	1.39	0.166
	Cue var	-0.052	0.03	2908.8	-1.73	0.084
	Cue SK (neg)	0.038	0.043	2907.7	0.88	0.378
	Cue SK (pos)	-0.005	0.043	2908.9	-0.11	0.909
	Cue mean x var	0.039	0.03	2915.3	1.31	0.192
	Stim int x cue mean	0.029	0.03	2907.1	0.95	0.344
Left NAc core	Stimulus Intensity	0.033	0.03	2947.9	1.1	0.273
	Cue mean	0.054	0.03	2948.4	1.81	0.07
	Cue var	**-0.104**	**0.03**	**2949.7**	**-3.47**	**0.001**
	Cue SK (neg)	0.019	0.042	2948.6	0.44	0.66
	Cue SK (pos)	-0.031	0.042	2949.1	-0.73	0.465
	Cue mean x var	**0.073**	**0.03**	**2948.3**	**2.43**	**0.015**
	Stim int x cue mean	-0.006	0.03	2948.6	-0.2	0.841
Right NAc core	Stimulus Intensity	0.045	0.03	2948.3	1.51	0.131
	Cue mean	0.021	0.03	2948.8	0.69	0.49
	Cue var	-0.02	0.03	2950.1	-0.67	0.5
	Cue SK (neg)	0.032	0.042	2948.9	0.76	0.445
	Cue SK (pos)	0.004	0.042	2949.5	0.09	0.929
	Cue mean x var	0.045	0.03	2948.6	1.5	0.133
	Stim int x cue mean	-0.002	0.03	2949	-0.06	0.956

Supplementary Table 8. Statistics for the effects on ROIs related to higher level visual processing. Abbreviations: var = variance; SK = skewness; neg = negative (vs. symmetric); pos = positive (vs. symmetric); stim int = stimulus intensity; IPS = intraparietal sulcus.

Region	Effect	Estimate	SE	DF	t	p
Left IPS	Stimulus Intensity	0.012	0.029	2958.7	0.40	0.691
	Cue mean	-0.054	0.029	2958.2	-1.84	0.066
	Cue var	-0.021	0.029	2958.8	-0.71	0.479
	Cue SK (neg)	-0.030	0.041	2958.6	-0.73	0.468
	Cue SK (pos)	-0.004	0.041	2958.5	-0.11	0.915
	Cue mean x var	0.029	0.029	2958.1	0.99	0.325
	Stim int x cue mean	-0.013	0.029	2958.1	-0.43	0.664
Right IPS	Stimulus Intensity	0.004	0.029	2956.7	0.14	0.891
	Cue mean	-0.052	0.029	2956.2	-1.79	0.074
	Cue var	-0.036	0.029	2956.8	-1.24	0.216
	Cue SK (neg)	-0.013	0.042	2956.6	-0.31	0.753
	Cue SK (pos)	0.000	0.041	2956.5	-0.01	0.991
	Cue mean x var	0.054	0.029	2956.2	1.86	0.064
	Stim int x cue mean	-0.015	0.029	2956.3	-0.52	0.605

Supplementary Table 9. Statistics for the effects on other pain processing ROIs. Abbreviations: var = variance; SK = skewness; neg = negative (vs. symmetric); pos = positive (vs. symmetric); stim int = stimulus intensity; aIns = anterior insula. Significant effects (uncorrected $p < .05$) are marked in bold.

Region	Effect	Estimate	SE	DF	t	p
Right aIns	**Stimulus Intensity**	**0.076**	**0.028**	**2904.4**	**2.68**	**0.007**
	Cue mean	0.018	0.029	295.0	0.61	0.540
	Cue var	0.008	0.028	2904.1	0.29	0.773
	Cue SK (neg)	0.007	0.040	2903.7	0.18	0.858
	Cue SK (pos)	0.071	0.040	2904.8	1.78	0.075
	Cue mean x var	0.002	0.028	2912.1	0.07	0.942
	Stim int x cue mean	-0.040	0.028	2903.2	-1.41	0.158
Left aIns	**Stimulus Intensity**	**0.093**	**0.029**	**2948.3**	**3.21**	**0.001**
	Cue mean	-0.016	0.029	2948.7	-0.54	0.588
	Cue var	0.002	0.029	2949.6	0.06	0.951
	Cue SK (neg)	0.024	0.041	2948.8	0.57	0.567
	Cue SK (pos)	0.045	0.041	2949.1	1.08	0.278
	Cue mean x var	-0.007	0.029	2948.6	-0.23	0.820
	Stim int x cue mean	-0.010	0.029	2948.9	-0.33	0.739
Right S1 hand	**Stimulus Intensity**	**0.117**	**0.026**	**2948.2**	**4.49**	**0.000**
	Cue mean	-0.007	0.026	2948.4	-0.27	0.788
	Cue var	-0.009	0.026	2948.8	-0.33	0.738
	Cue SK (neg)	0.015	0.037	2948.4	0.40	0.689
	Cue SK (pos)	0.036	0.037	2948.6	0.99	0.324
	Cue mean x var	0.018	0.026	2948.4	0.67	0.500
	Stim int x cue mean	-0.010	0.026	2948.5	-0.37	0.709
Left S1 hand	**Stimulus Intensity**	**0.133**	**0.027**	**2908.5**	**5.00**	**0.000**
	Cue mean	-0.033	0.027	357.6	-1.21	0.225
	Cue var	-0.012	0.027	2907.8	-0.46	0.645
	Cue SK (neg)	0.034	0.038	2907.6	0.90	0.370
	Cue SK (pos)	0.024	0.038	2908.5	0.63	0.527
	Cue mean x var	-0.020	0.027	2916.3	-0.76	0.445
	Stim int x cue mean	-0.009	0.027	2907.2	-0.34	0.736

Supplementary Table 10. Statistics for the effects on other visual processing ROIs. Abbreviations: var = variance; SK = skewness; neg = negative (vs. symmetric); pos = positive (vs. symmetric); stim int = stimulus intensity. Significant effects (uncorrected $p < .05$) are marked in bold.

Region	Effect	Estimate	SE	DF	t	p
	Stimulus Intensity	0.041	0.027	2958	1.54	0.124
	Cue mean	-0.014	0.027	2957.7	-0.54	0.590
	Cue var	0.014	0.027	2958	0.54	0.590
Right V3A	**Cue SK (neg)**	**-0.087**	**0.038**	**2957.9**	**-2.30**	**0.021**
	Cue SK (pos)	-0.040	0.038	2957.9	-1.05	0.292
	Cue mean x var	0.000	0.027	2957.7	0.02	0.987
	Stim int x cue mean	-0.003	0.027	2957.7	-0.11	0.911
	Stimulus Intensity	0.043	0.028	2955.5	1.57	0.115
	Cue mean	-0.012	0.028	2955.2	-0.45	0.653
	Cue var	-0.003	0.028	2955.5	-0.10	0.920
Left V3A	**Cue SK (neg)**	**-0.101**	**0.039**	**2955.4**	**-2.57**	**0.010**
	Cue SK (pos)	-0.052	0.039	2955.3	-1.33	0.184
	Cue mean x var	-0.022	0.028	2955.1	-0.82	0.415
	Stim int x cue mean	-0.004	0.028	2955.2	-0.13	0.898
	Stimulus Intensity	0.033	0.029	2961.9	1.13	0.260
	Cue mean	-0.046	0.029	2961.4	-1.58	0.114
	Cue var	-0.013	0.029	2962	-0.44	0.657
Right V3B	Cue SK (neg)	-0.046	0.041	2961.8	-1.13	0.260
	Cue SK (pos)	-0.029	0.041	2961.7	-0.71	0.476
	Cue mean x var	0.040	0.029	2961.4	1.39	0.164
	Stim int x cue mean	0.012	0.029	2961.4	0.42	0.672
	Stimulus Intensity	0.007	0.028	2960.9	0.24	0.811
	Cue mean	-0.019	0.028	2960.5	-0.68	0.494
	Cue var	-0.024	0.028	2960.8	-0.88	0.379
Left V3B	Cue SK (neg)	-0.055	0.039	2960.7	-1.40	0.163
	Cue SK (pos)	-0.023	0.039	2960.6	-0.58	0.562
	Cue mean x var	-0.003	0.028	2960.4	-0.11	0.911
	Stim int x cue mean	0.018	0.028	2960.5	0.64	0.523
	Stimulus Intensity	0.032	0.026	2946.2	1.23	0.219
	Cue mean	-0.022	0.026	2946	-0.85	0.393
	Cue var	-0.046	0.026	2946.2	-1.76	0.079
Right V3CD	Cue SK (neg)	-0.064	0.037	2946.2	-1.74	0.083
	Cue SK (pos)	-0.052	0.037	2946.1	-1.41	0.160
	Cue mean x var	0.031	0.026	2946	1.19	0.234
	Stim int x cue mean	0.021	0.026	2946	0.81	0.416
	Stimulus Intensity	0.001	0.026	2960.6	0.06	0.955
	Cue mean	-0.015	0.026	2960.3	-0.56	0.575
	Cue var	-0.038	0.026	2960.6	-1.48	0.139
Left V3CD	Cue SK (neg)	-0.020	0.037	2960.5	-0.54	0.588
	Cue SK (pos)	-0.035	0.037	2960.4	-0.94	0.346
	Cue mean x var	0.013	0.026	2960.3	0.51	0.609
	Stim int x cue mean	-0.008	0.026	2960.3	-0.30	0.765
	Stimulus Intensity	0.001	0.029	2952.9	0.04	0.968
	Cue mean	0.008	0.029	2952.4	0.26	0.792
	Cue var	-0.021	0.029	2952.9	-0.73	0.466
Right V4t	Cue SK (neg)	-0.062	0.040	2952.7	-1.52	0.128
	Cue SK (pos)	-0.042	0.040	2952.6	-1.05	0.293
	Cue mean x var	0.048	0.029	2952.4	1.67	0.095
	Stim int x cue mean	0.002	0.029	2952.4	0.05	0.957
	Stimulus Intensity	-0.002	0.027	2961.3	-0.07	0.945
	Cue mean	-0.022	0.027	2961.1	-0.84	0.398
	Cue var	-0.041	0.027	2961.4	-1.54	0.125
Left V4t	Cue SK (neg)	-0.062	0.038	2961.3	-1.64	0.101
	Cue SK (pos)	-0.056	0.038	2961.2	-1.48	0.138
	Cue mean x var	0.020	0.027	2961.1	0.73	0.463
	Stim int x cue mean	0.026	0.027	2961.1	0.97	0.334

Right ventro-medial V1	Stimulus Intensity	0.023	0.030	2955.6	0.79	0.432
	Cue mean	0.020	0.030	2954.8	0.66	0.510
	Cue var	-0.013	0.030	2955.6	-0.43	0.668
	Cue SK (neg)	-0.035	0.042	2955.4	-0.82	0.413
	Cue SK (pos)	-0.012	0.042	2955.2	-0.28	0.780
	Cue mean x var	-0.018	0.030	2954.7	-0.61	0.542
	Stim int x cue mean	0.005	0.030	2954.9	0.18	0.856
Left ventro-medial V1	Stimulus Intensity	0.007	0.030	2915.6	0.25	0.806
	Cue mean	-0.017	0.031	330.5	-0.55	0.585
	Cue var	0.033	0.030	2915	1.09	0.275
	Cue SK (neg)	-0.026	0.043	2915.2	-0.62	0.537
	Cue SK (pos)	0.005	0.043	2914.6	0.12	0.903
	Cue mean x var	-0.017	0.030	2916.3	-0.56	0.577
	Stim int x cue mean	0.014	0.030	2917.3	0.48	0.632
Right ventro-medial V2	Stimulus Intensity	0.018	0.030	234.8	0.58	0.564
	Cue mean	-0.005	0.030	266.1	-0.18	0.857
	Cue var	0.013	0.029	2875.1	0.45	0.650
	Cue SK (neg)	-0.068	0.040	2874.7	-1.68	0.094
	Cue SK (pos)	-0.039	0.040	2880.5	-0.96	0.339
	Cue mean x var	-0.026	0.029	2875.7	-0.91	0.362
	Stim int x cue mean	-0.005	0.029	2877.1	-0.16	0.874
Left ventro-medial V2	Stimulus Intensity	-0.021	0.029	2959.2	-0.73	0.466
	Cue mean	-0.026	0.029	2958.7	-0.91	0.360
	Cue var	-0.020	0.029	2959.2	-0.70	0.486
	Cue SK (neg)	-0.006	0.041	2959	-0.16	0.876
	Cue SK (pos)	-0.024	0.041	2958.9	-0.58	0.564
	Cue mean x var	-0.011	0.029	2958.6	-0.38	0.702
	Stim int x cue mean	-0.008	0.029	2958.7	-0.26	0.793
Right ventro-medial V3	Stimulus Intensity	0.033	0.028	2911	1.16	0.247
	Cue mean	-0.014	0.029	319.8	-0.48	0.629
	Cue var	0.016	0.028	2910.1	0.55	0.582
	Cue SK (neg)	-0.078	0.040	2910.3	-1.93	0.053
	Cue SK (pos)	-0.046	0.040	2910.5	-1.15	0.249
	Cue mean x var	0.000	0.028	2912.5	0.02	0.987
	Stim int x cue mean	-0.014	0.028	2913	-0.49	0.624
Left ventro-medial V3	Stimulus Intensity	0.027	0.028	2962.7	0.98	0.326
	Cue mean	-0.027	0.028	2962.5	-0.97	0.330
	Cue var	-0.012	0.028	2962.8	-0.45	0.651
	Cue SK (neg)	-0.057	0.039	2962.8	-1.45	0.147
	Cue SK (pos)	-0.033	0.039	2962.6	-0.84	0.403
	Cue mean x var	0.006	0.028	2962.4	0.23	0.819
	Stim int x cue mean	-0.019	0.028	2962.5	-0.70	0.482

References (Supplementary Information)

1. Glasser, M. F. *et al.* A multi-modal parcellation of human cerebral cortex. *Nature* **536**, 171–178 (2016).
2. Tian, Y., Margulies, D. S., Breakspear, M. & Zalesky, A. Topographic organization of the human subcortex unveiled with functional connectivity gradients. *Nat. Neurosci.* **23**, 1421–1432 (2020).
3. Krauth, A. *et al.* A mean three-dimensional atlas of the human thalamus: generation from multiple histological data. *Neuroimage* **49**, 2053–2062 (2010).